

Electronic Supplementary Information for:

Nafion vs. Fumion: Impact of Ionomers on the
Alkaline Oxygen Evolution Reaction

*Mairead R. Brownell, Kenta Kawashima, Ashutosh Rana, Hugo Celio, Chikaodili E. Chukwuneke,
James H. Nguyen, Nathaniel R. Miller, Jeffrey E. Dick*, C. Buddie Mullins**

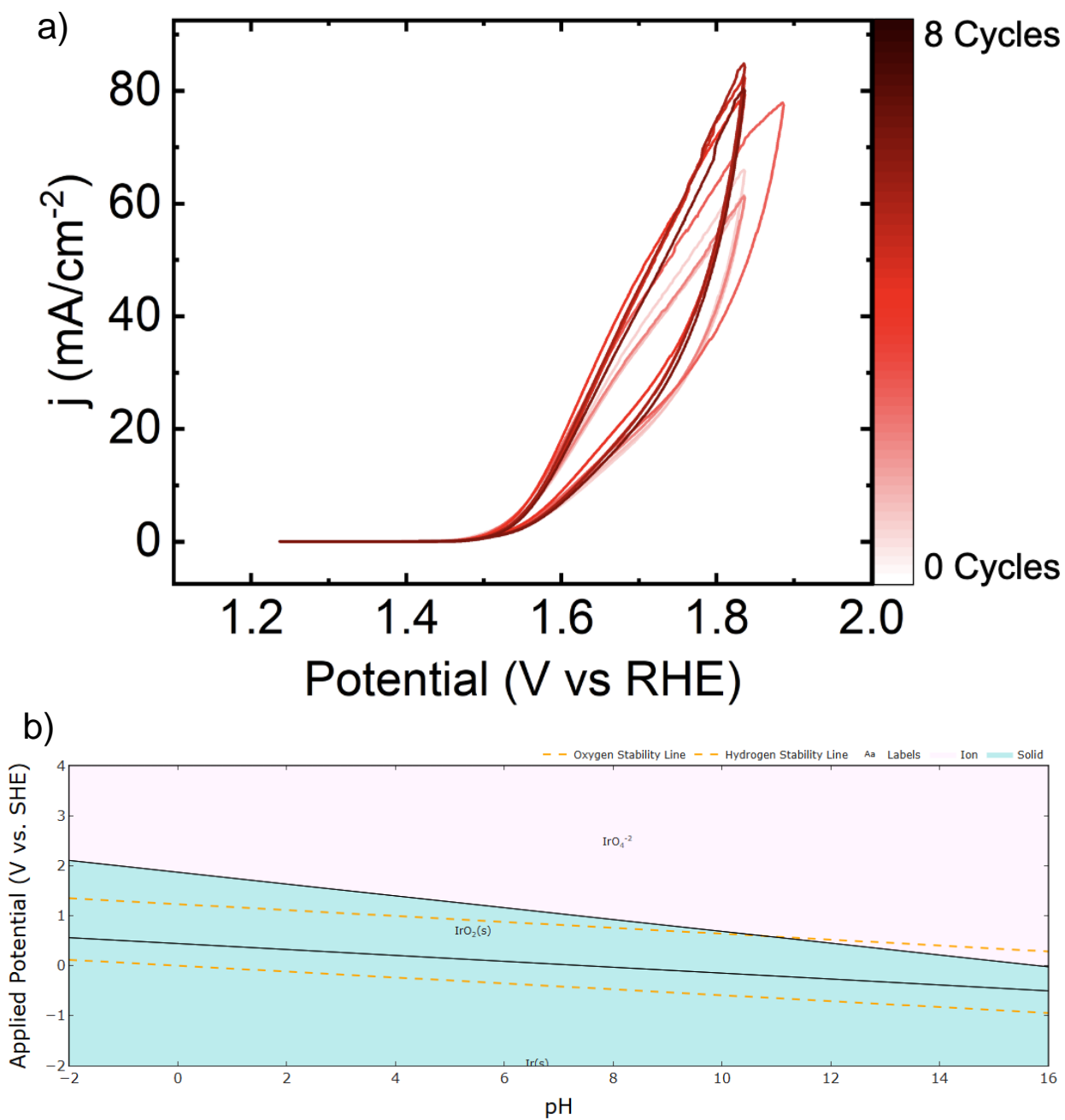


Fig. S1. (a) Cyclic voltammetry plots showing the activation of Ir/C to IrO₂ in 1 M KOH (measured at a scan rate of 5 mV·s⁻¹). The sample seems to be fully activated after about four cycles, as is evident by the darker curves in the plot. (b) The Pourbaix diagram of iridium generated by materials project.¹⁻⁵

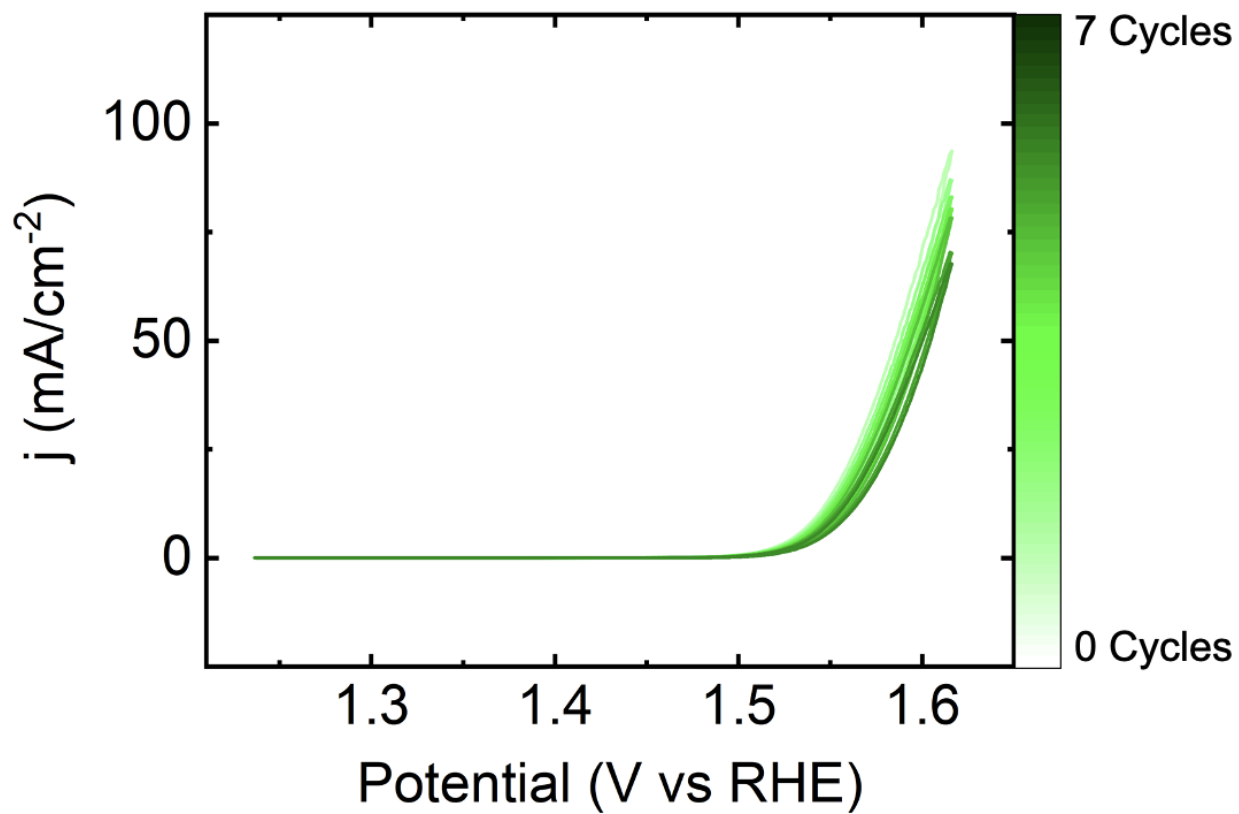


Fig. S2. Cyclic voltammetry plots showing the degradation of the electrode employing mixed ionomer in 1 M KOH (measured at a scan rate of $5 \text{ mV} \cdot \text{s}^{-1}$).

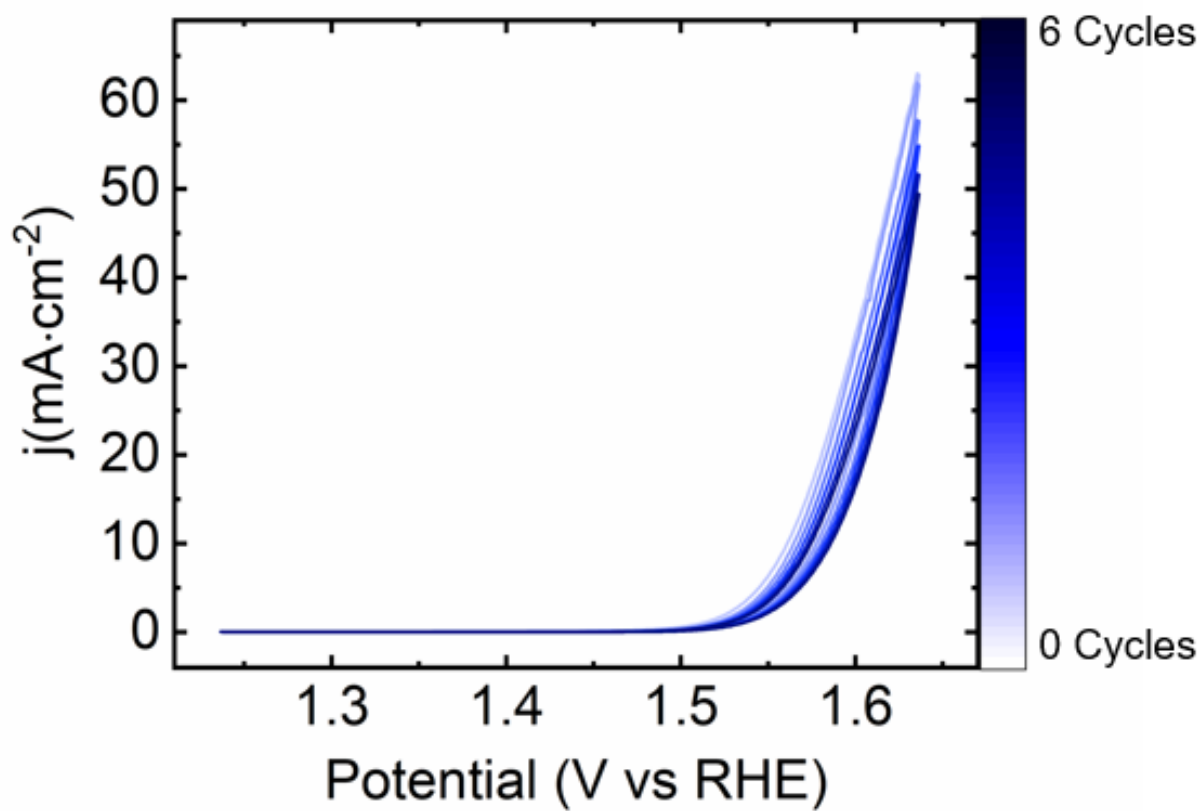


Fig. S3. Cyclic voltammetry plots showing the degradation of the electrode employing Fumion ionomer in 1 M KOH (measured at a scan rate of $5 \text{ mV}\cdot\text{s}^{-1}$).

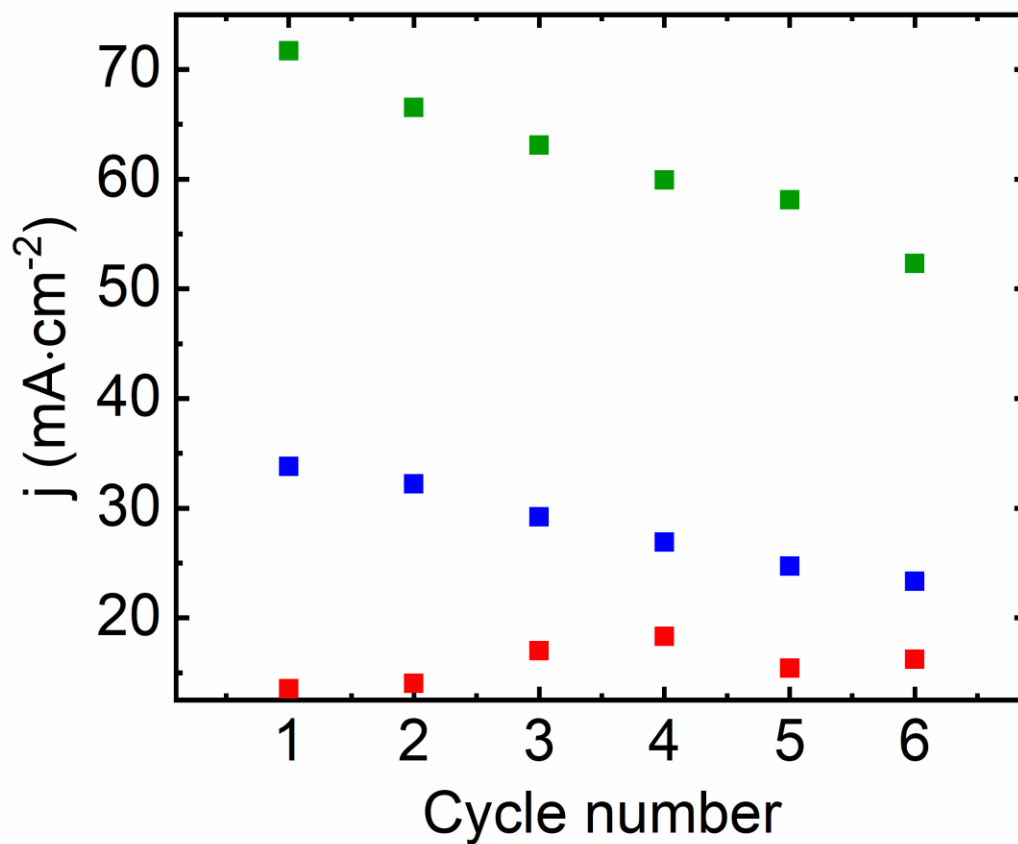


Fig. S4. Current density at 1.6 V for each cyclic voltammogram of electrodes containing Nafion, Fumion, and 1:1 mixed binder. Experiments were performed in 1 M KOH using a scan rate of 5 $\text{mV}\cdot\text{s}^{-1}$.

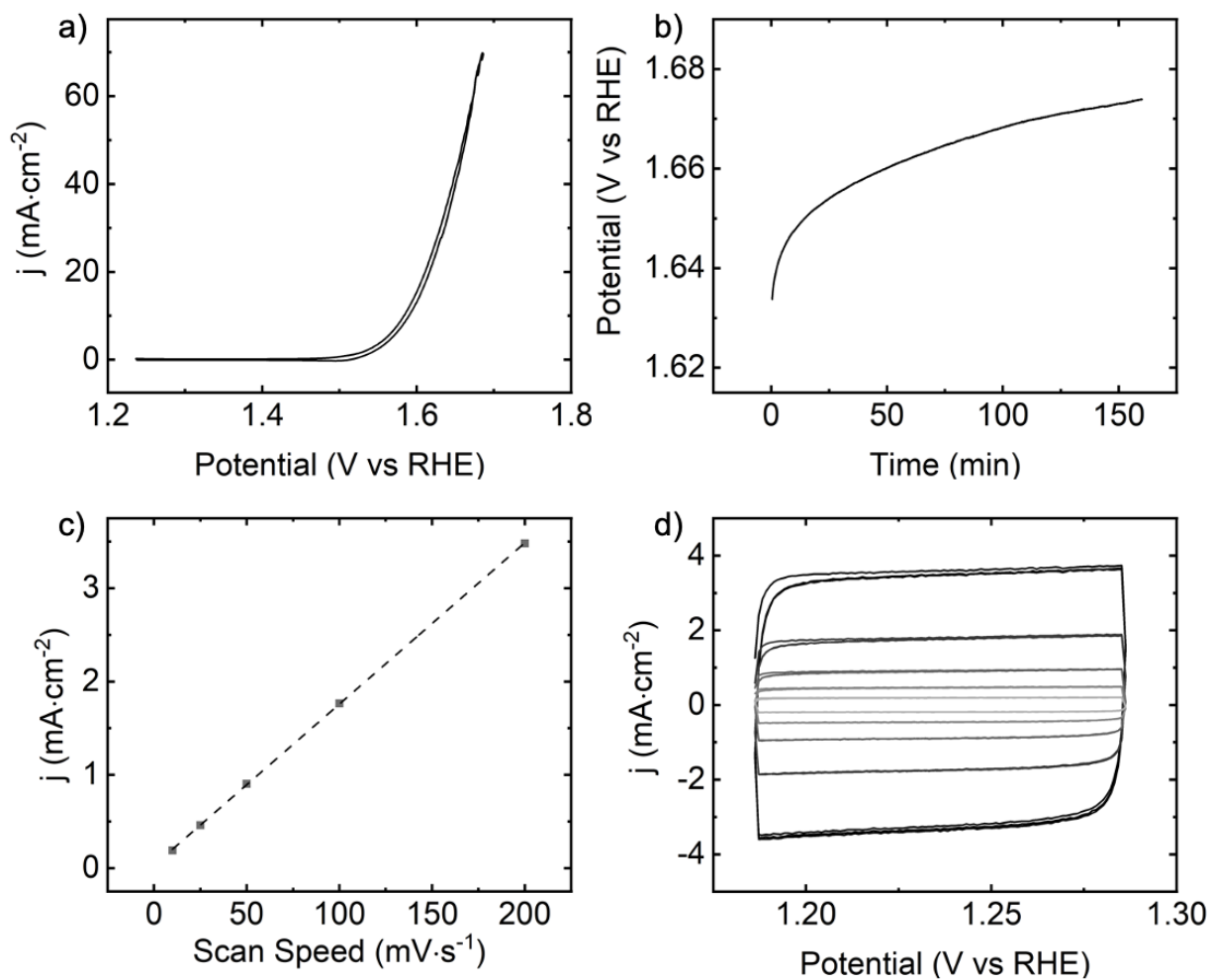


Fig. S5. Baseline electrochemical data of IrO₂, including a) CV (measured with a scan rate of 5 mV·s⁻¹), b) CP (10 mA·cm⁻²), c) analyzed ECSA data, and d) CVs for ECSA (scan rates ranging from 10 mV·s⁻¹) measured in 1 M KOH.

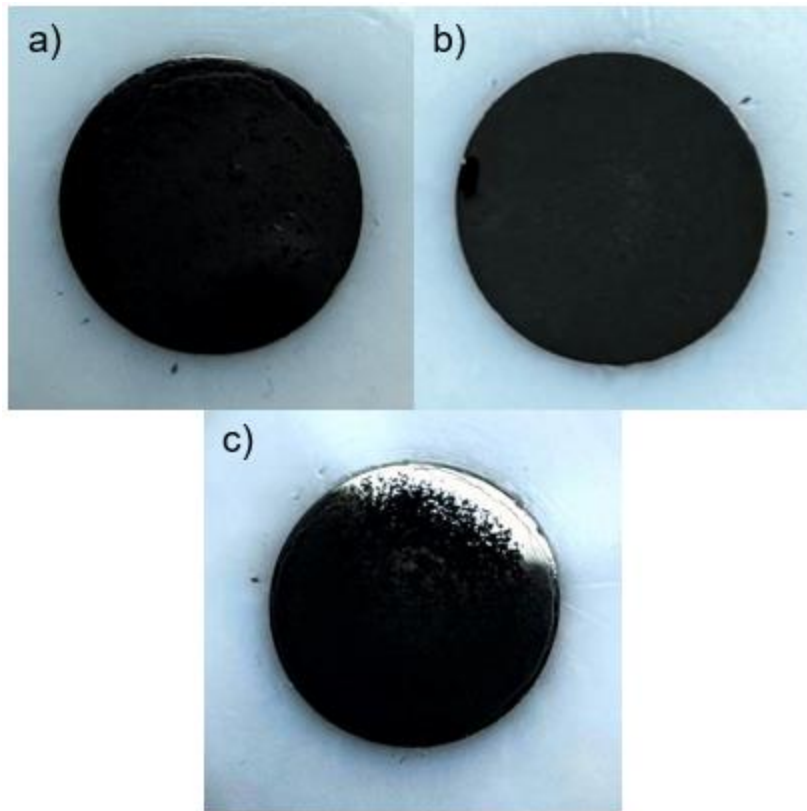


Fig. S6. Images of the electrodes fabricated with a) Nafion, b) Fumion, and c) mixed binders.

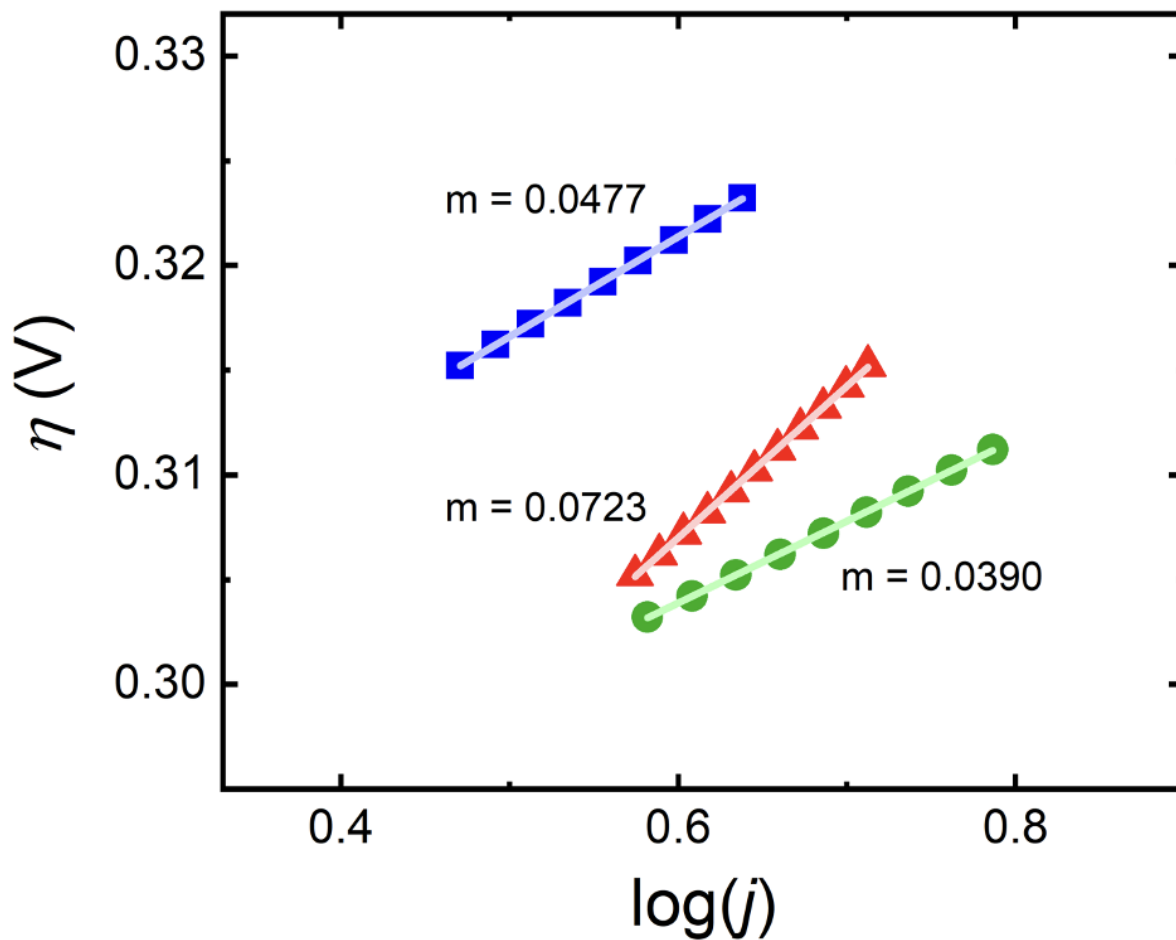


Fig. S7. Tafel slopes of the samples using Nafion (red), Fumion (blue), and mixed ionomer (green) as a binder, calculated from the Tafel region of LSV measurements observed in 1 M KOH using a scan rate of $5 \text{ mV} \cdot \text{s}^{-1}$. Current density, j , is in units of $\text{mA} \cdot \text{cm}^{-2}$ while slopes are reported in units of $\text{V} \cdot \text{dec}^{-1}$.

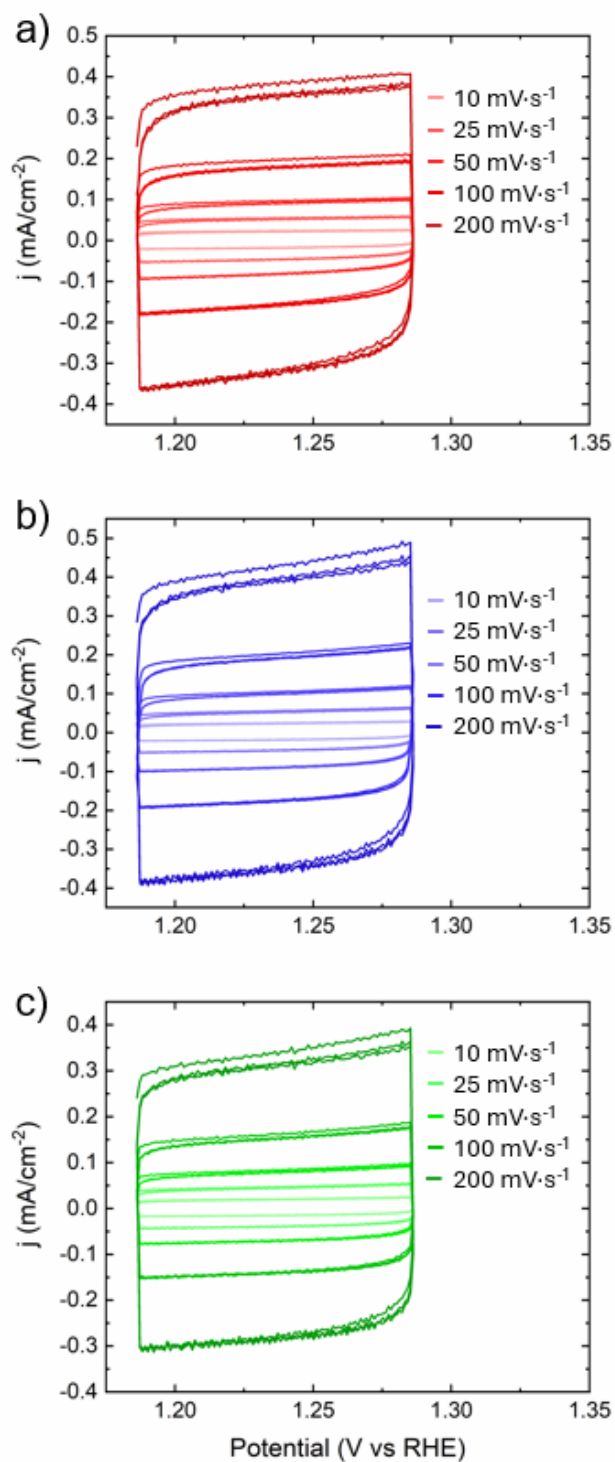


Fig. S8. Initial cycling data used to calculate double layer capacitance and ECSA of electrodes containing (a) Nafion, (b) Fumion, and (c) mixed ionomer with scan rates ranging from 10 mV·s⁻¹ to 200 mV·s⁻¹.

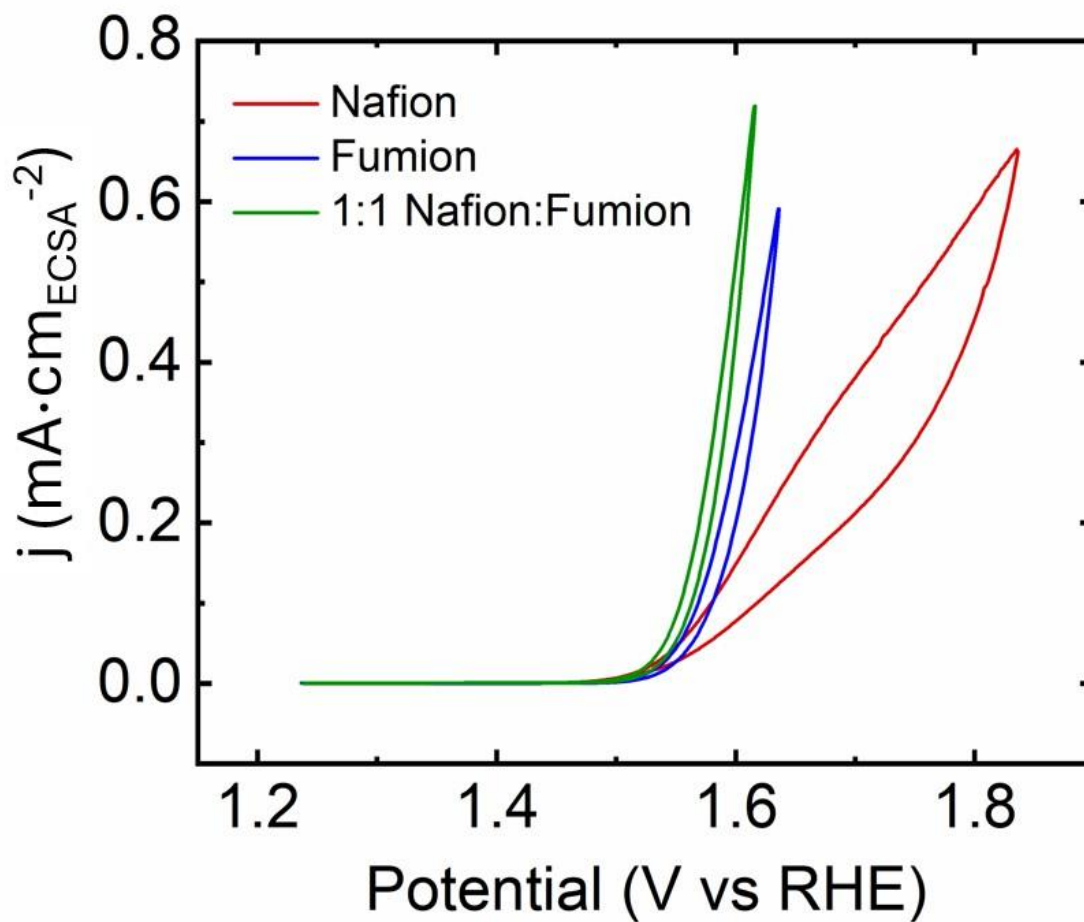


Fig. S9. CV measurements conducted on Ir/C electrocatalysts containing Nafion, Fumion, and 1:1 Nafion:Fumion ionomer. Current density is reported using electrochemically active surface area determined from capacitive current.

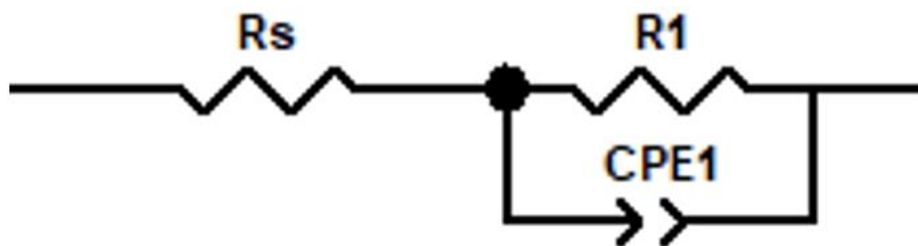


Fig. S10. Representative Randall's circuit used for fitting EIS spectra for determination of charge transfer resistance (R_1) and double layer capacitance ($CPE1$).

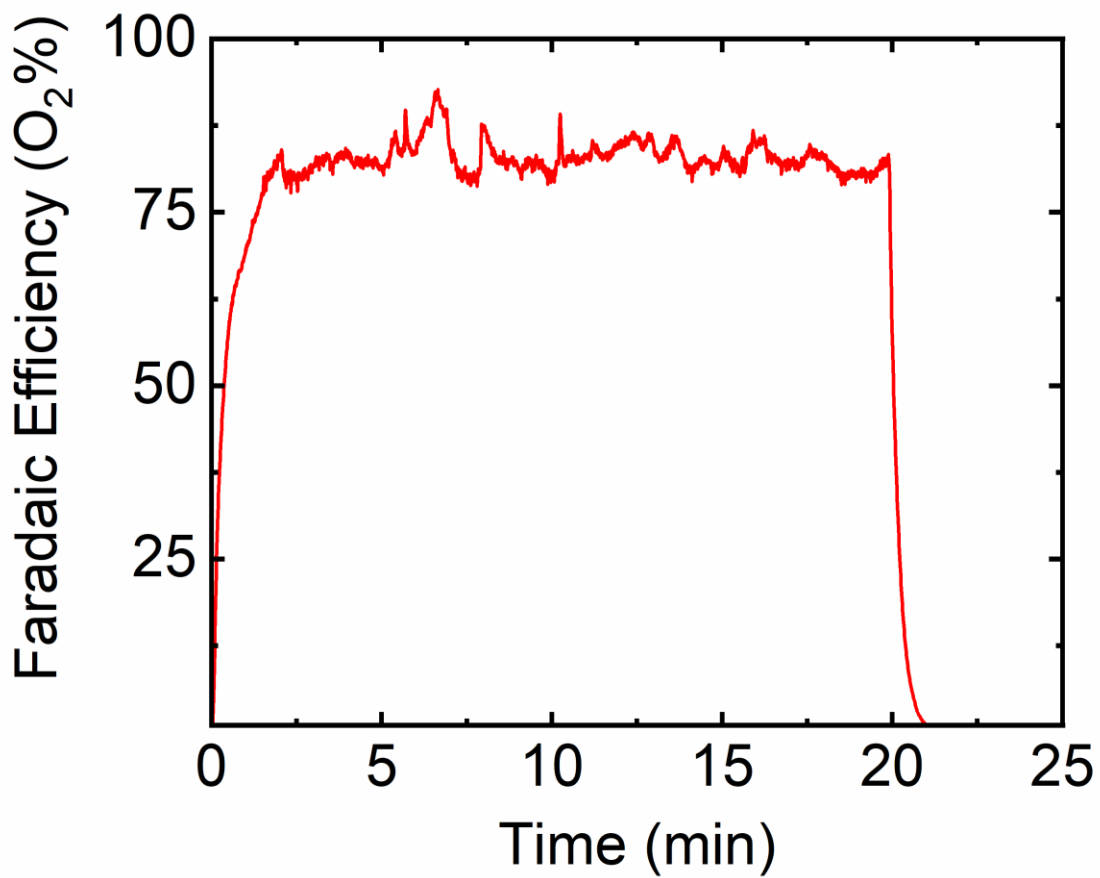


Fig. S11. ECMS measurement of oxygen evolved during chronopotentiometry measurements measured in 1 M KOH and collected at $0.5 \text{ mA}\cdot\text{cm}^{-2}$ for samples containing Nafion. Oxygen evolved was normalized to total overall current applied to obtain *in situ* Faradaic efficiency of the OER.

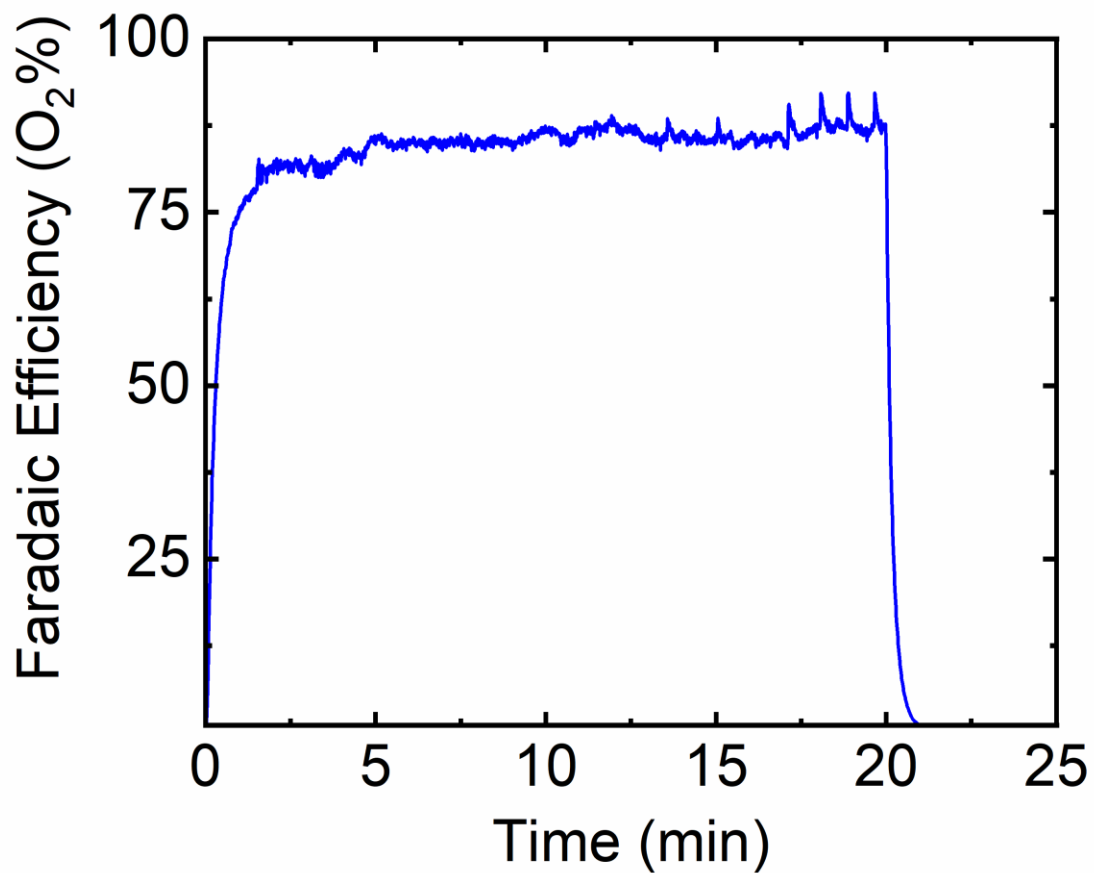


Fig. S12. ECMS measurement of oxygen evolved during chronopotentiometry measurements measured in 1 M KOH and collected at $0.5 \text{ mA}\cdot\text{cm}^{-2}$ for samples containing Fumion. Oxygen evolved was normalized to total overall current applied to obtain *in situ* Faradaic efficiency of the OER.

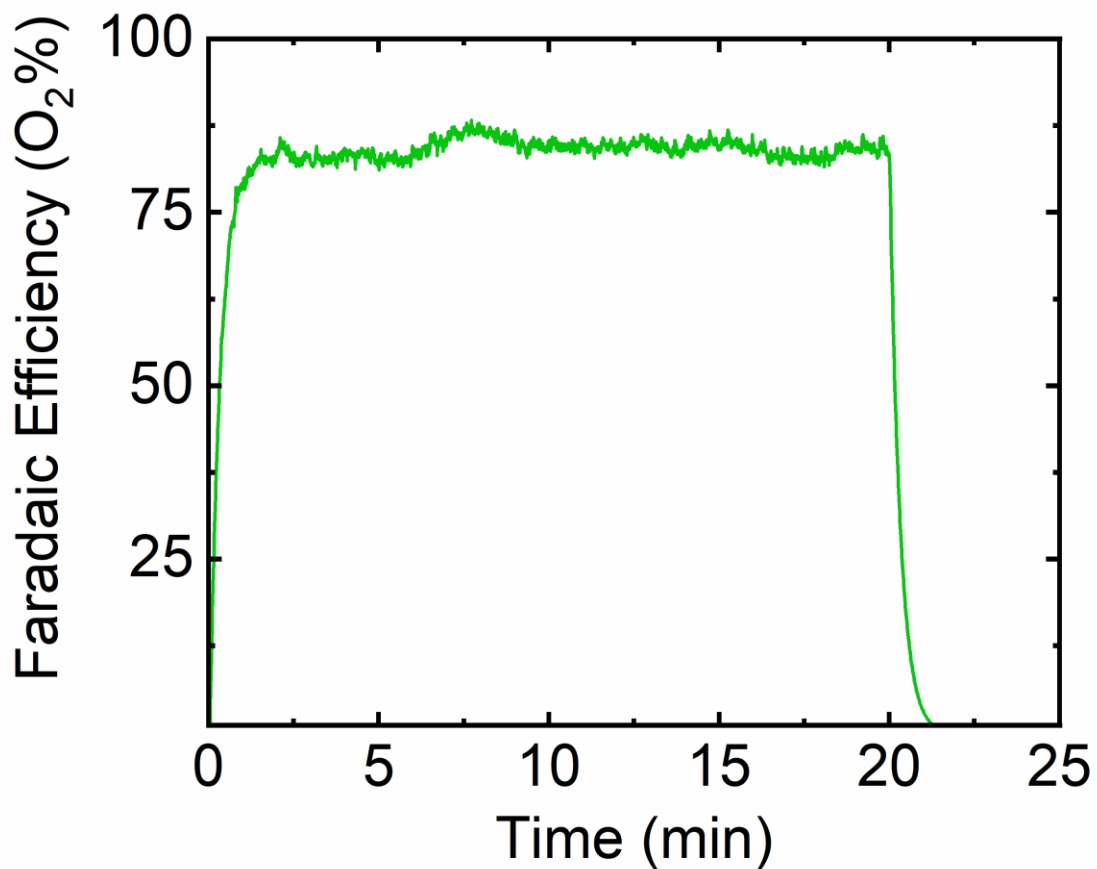


Fig. S13. ECMS measurement of oxygen evolved during chronopotentiometry measurements measured in 1 M KOH and collected at $0.5 \text{ mA}\cdot\text{cm}^{-2}$ for samples containing mixed ionomer. Oxygen evolved was normalized to total overall current applied to obtain *in situ* Faradaic efficiency of the OER.

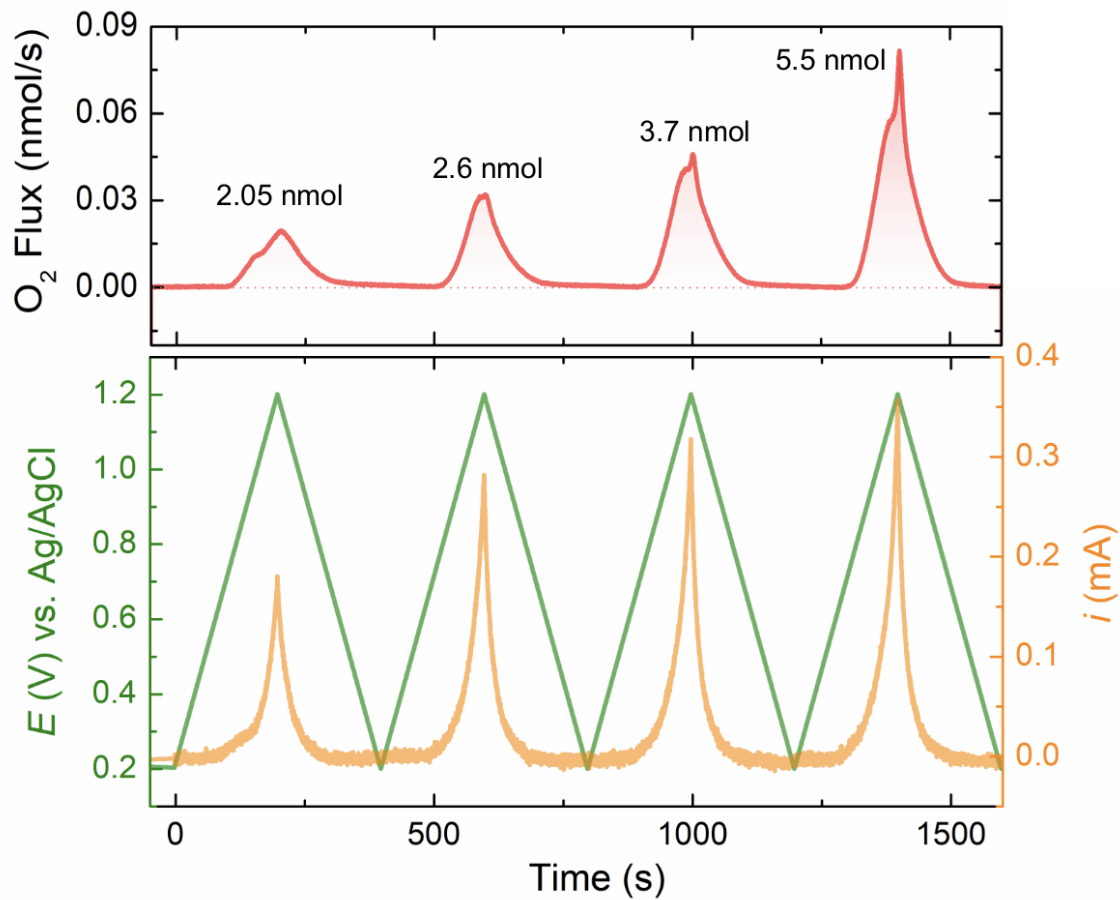


Fig. S14. Oxygen evolved during cyclic voltammetry measurements of a bare glassy carbon electrode in 1 M KOH using a scan rate of $5 \text{ mV} \cdot \text{s}^{-1}$.

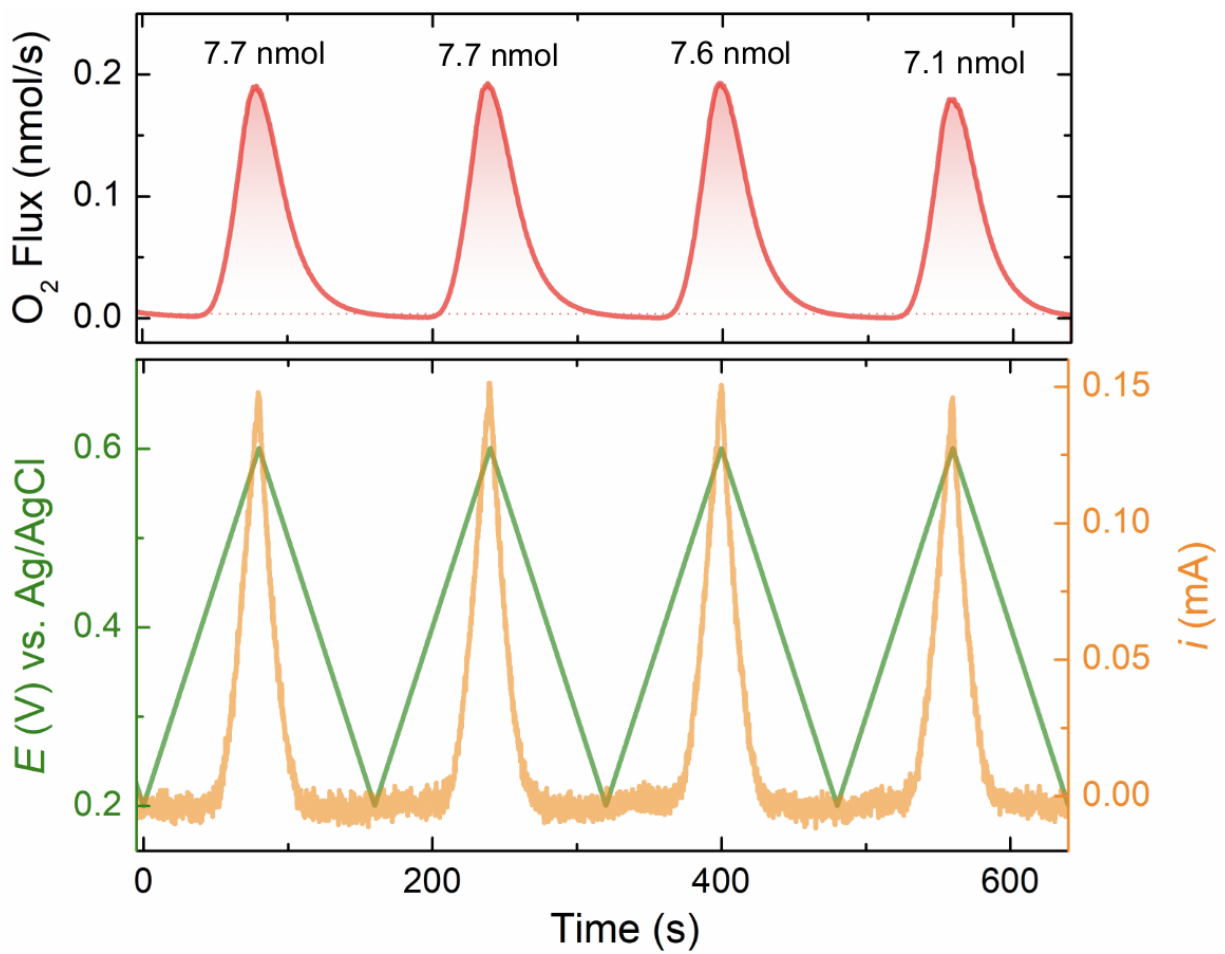


Fig. S15. Oxygen evolved during cyclic voltammetry measurements of the electrode containing Fumion in 1 M KOH using a scan rate of $5 \text{ mV} \cdot \text{s}^{-1}$.

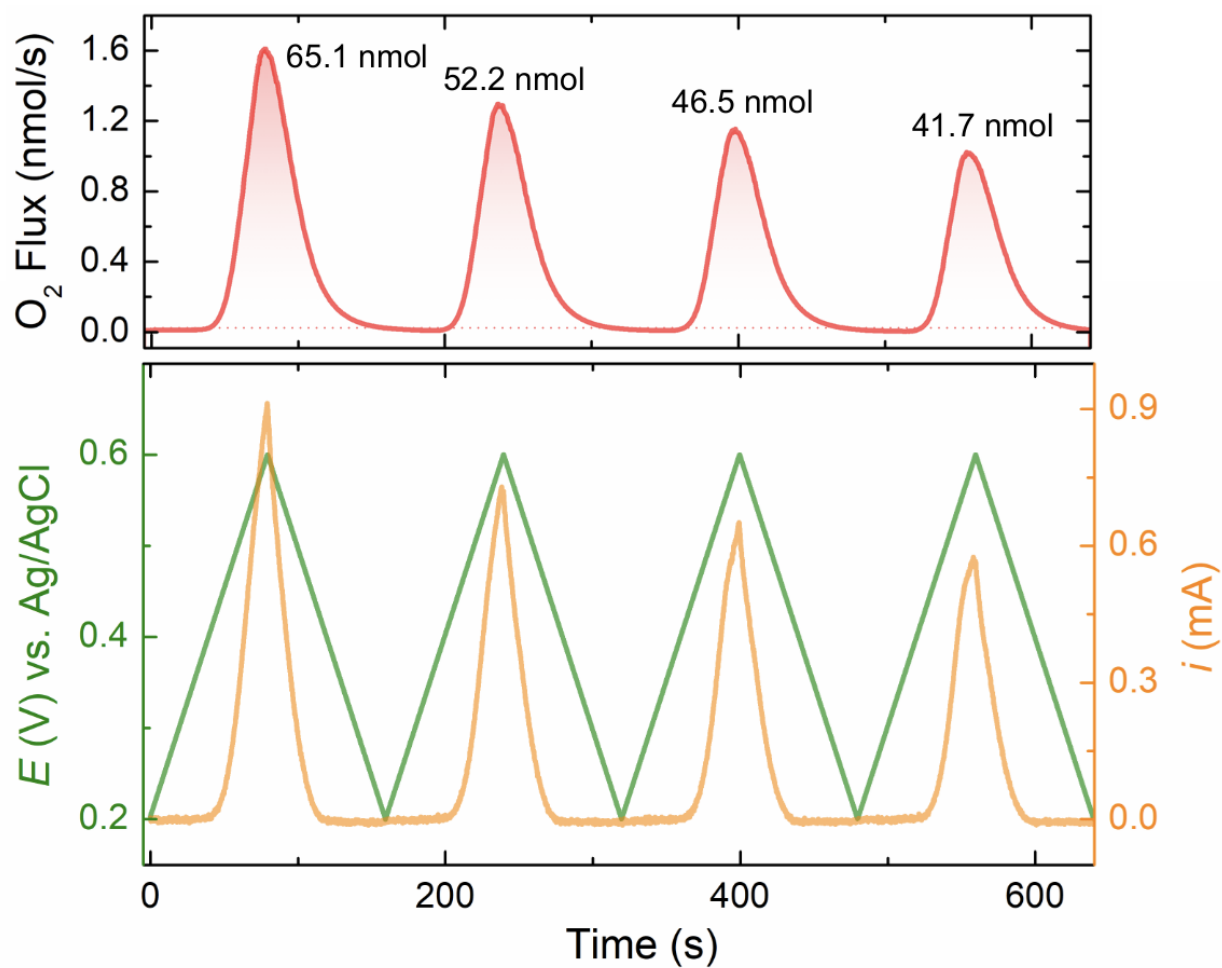


Fig. S16. Oxygen evolved during cyclic voltammetry measurements of the electrode containing mixed ionomer in 1 M KOH using a scan rate of $5 \text{ mV} \cdot \text{s}^{-1}$.

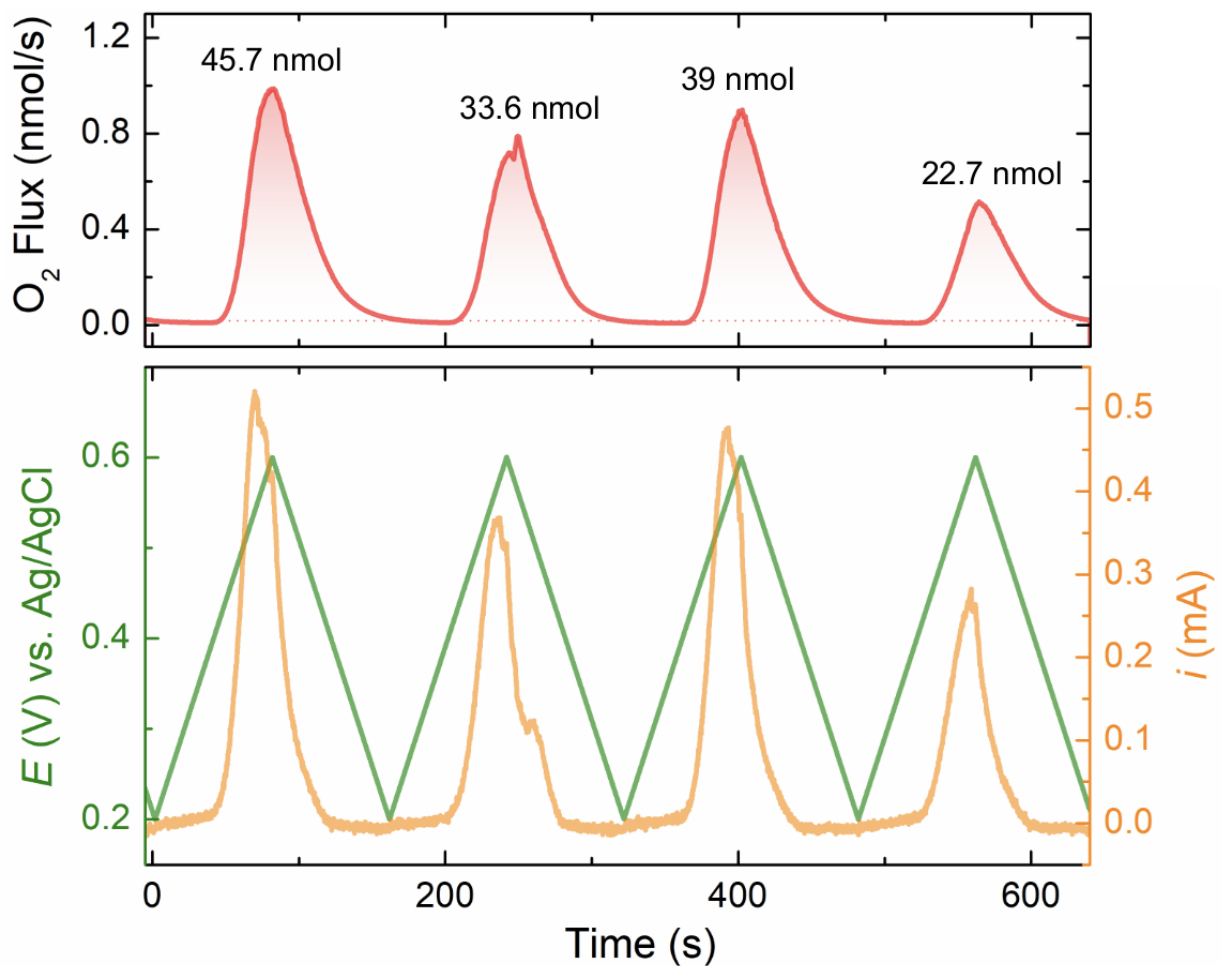


Fig. S17. Oxygen evolved during cyclic voltammetry measurements of the electrode containing Nafion in 1 M KOH using a scan rate of $5 \text{ mV} \cdot \text{s}^{-1}$.

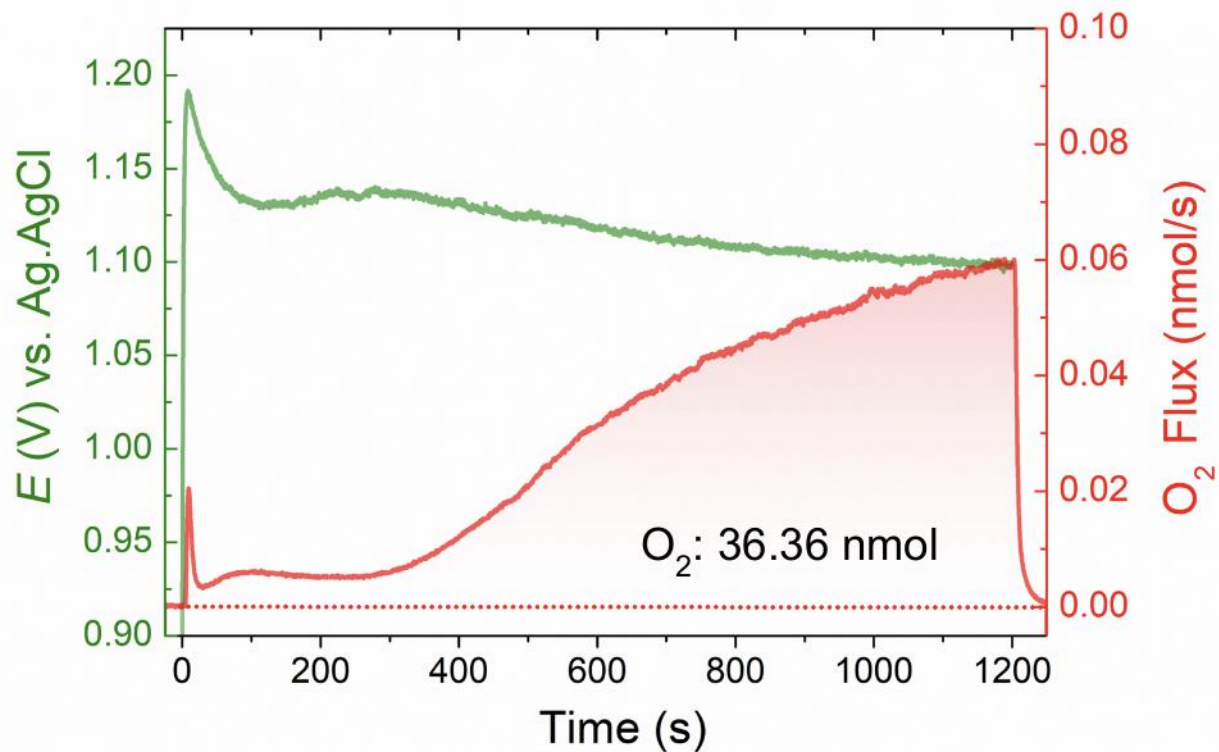


Fig. S18. Oxygen evolved during chronopotentiometry measurements of the electrode containing Nafion in 1 M KOH using a current density of $0.5 \text{ mA} \cdot \text{cm}^{-2}$.

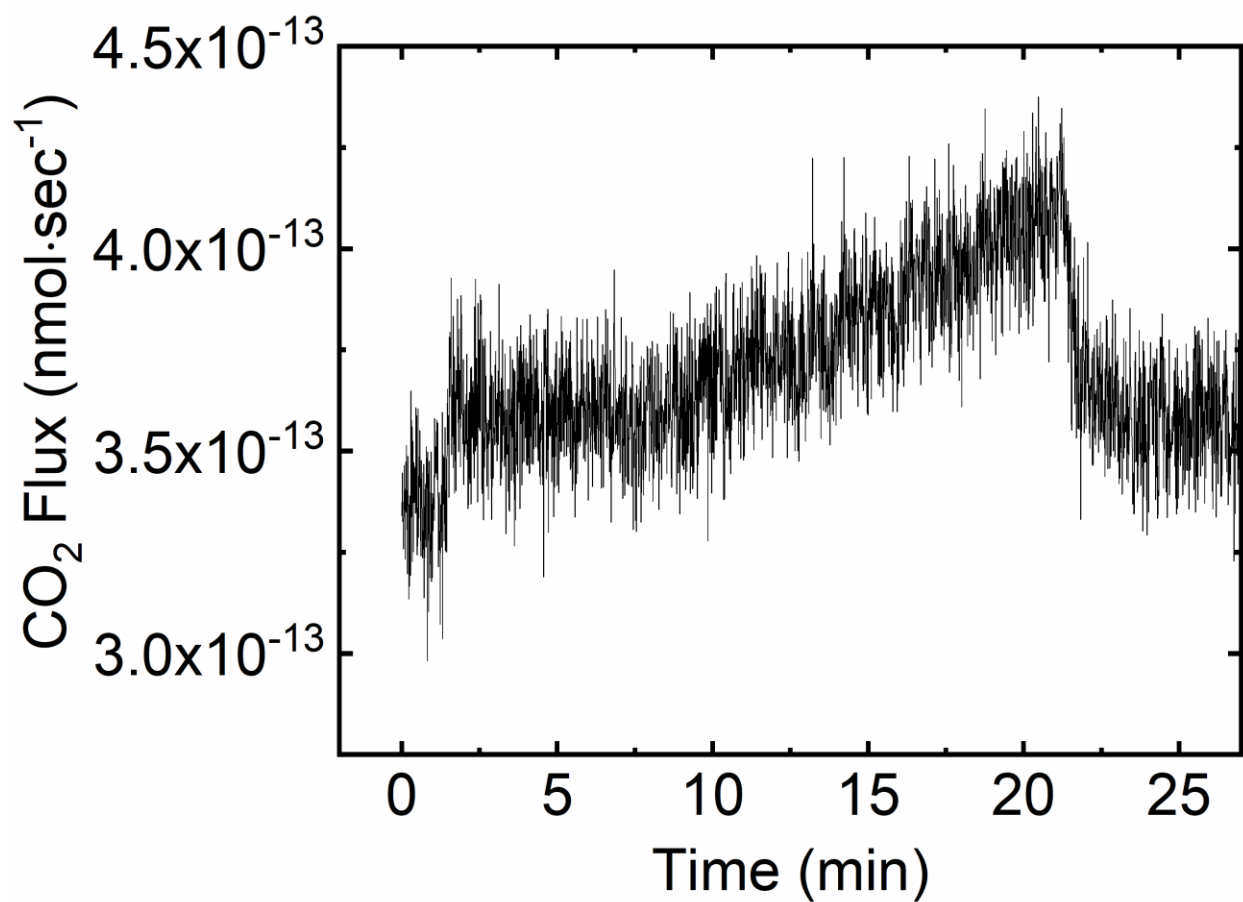


Figure S19. Carbon dioxide evolved during chronopotentiometry measurements of of a bare glassy carbon electrode in 1 M KOH using a current density of 0.5 mA·cm⁻².

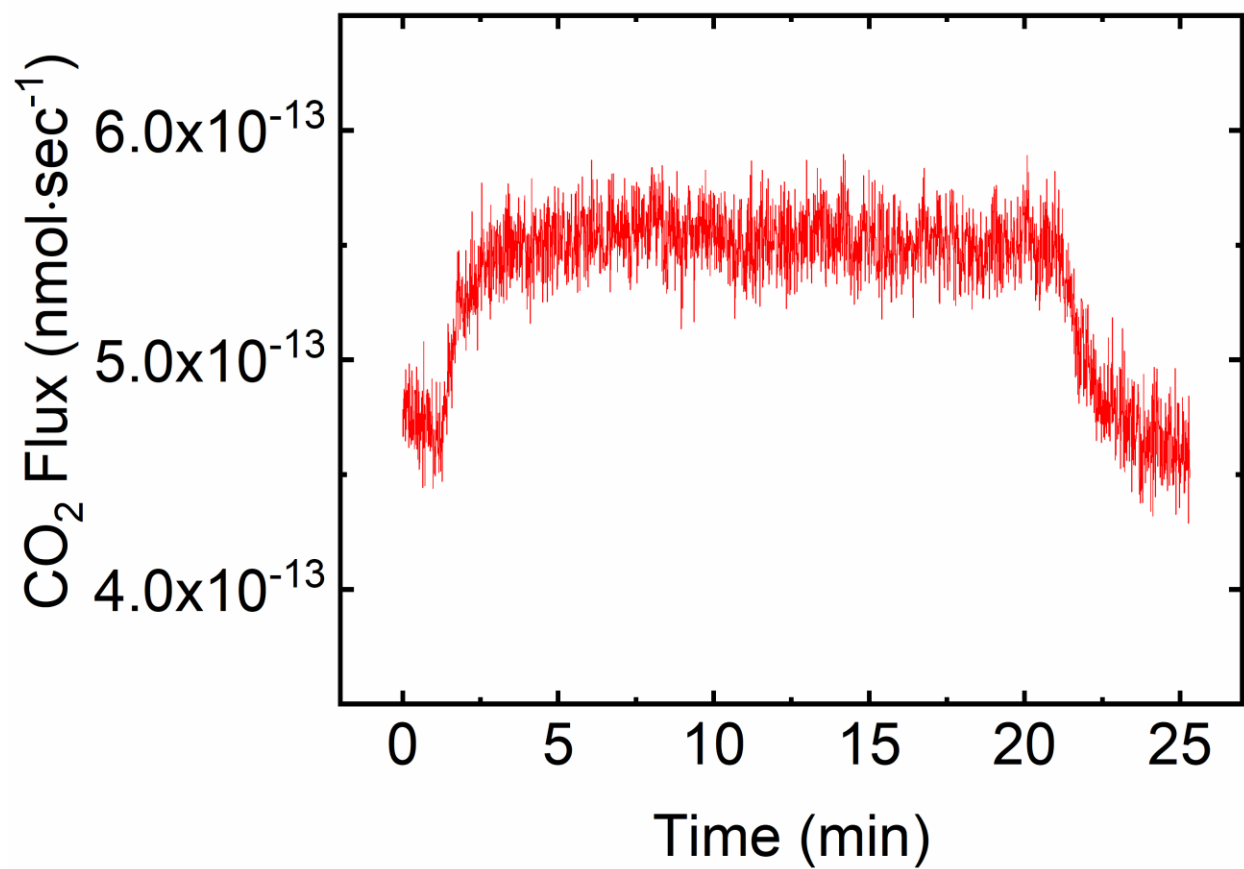


Figure S20. Carbon dioxide evolved during chronopotentiometry measurements of the electrode containing Nafion in 1 M KOH using a current density of 0.5 mA·cm⁻².

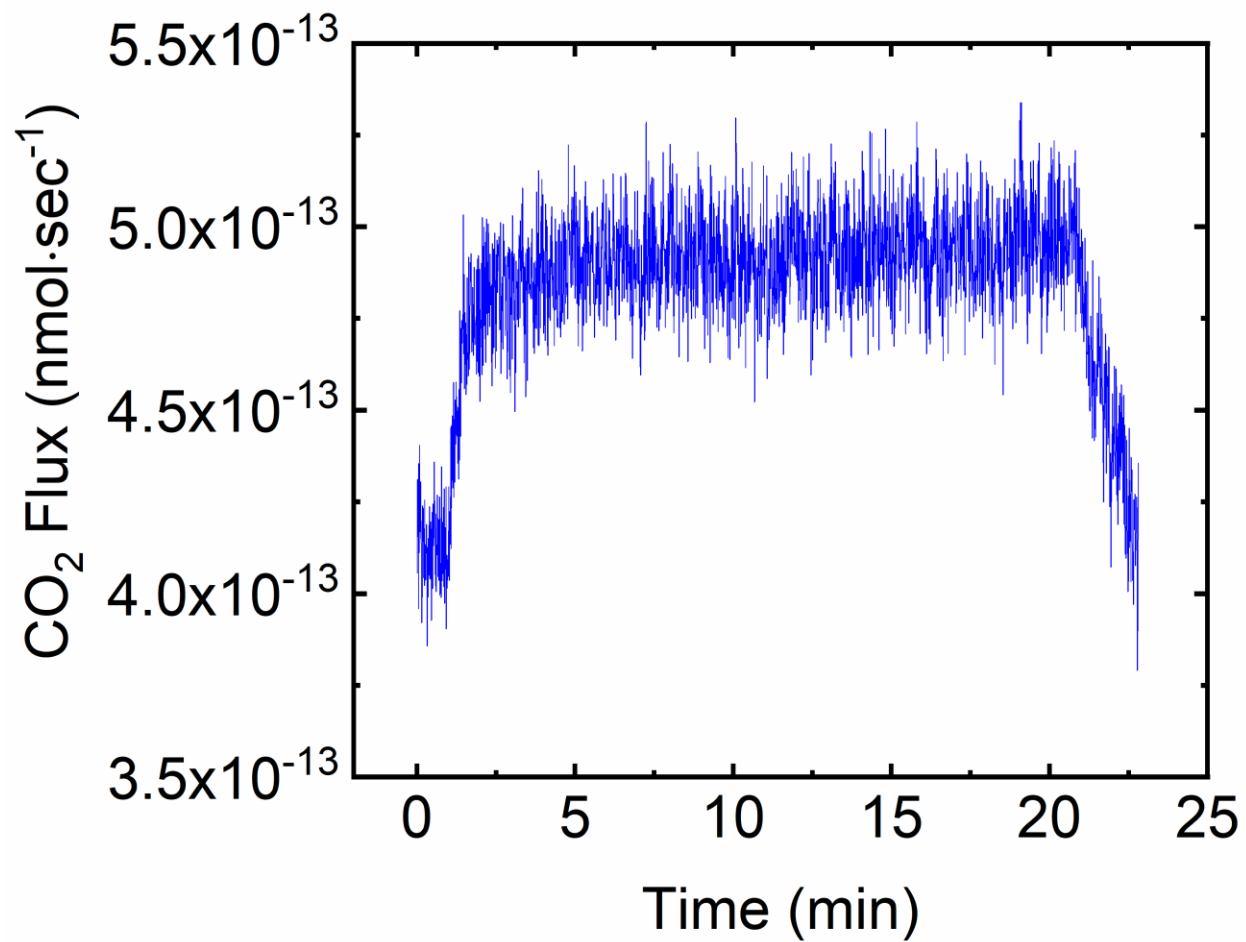


Figure S21. Carbon dioxide evolved during chronopotentiometry measurements of the electrode containing Fumion in 1 M KOH using a current density of 0.5 mA·cm⁻².

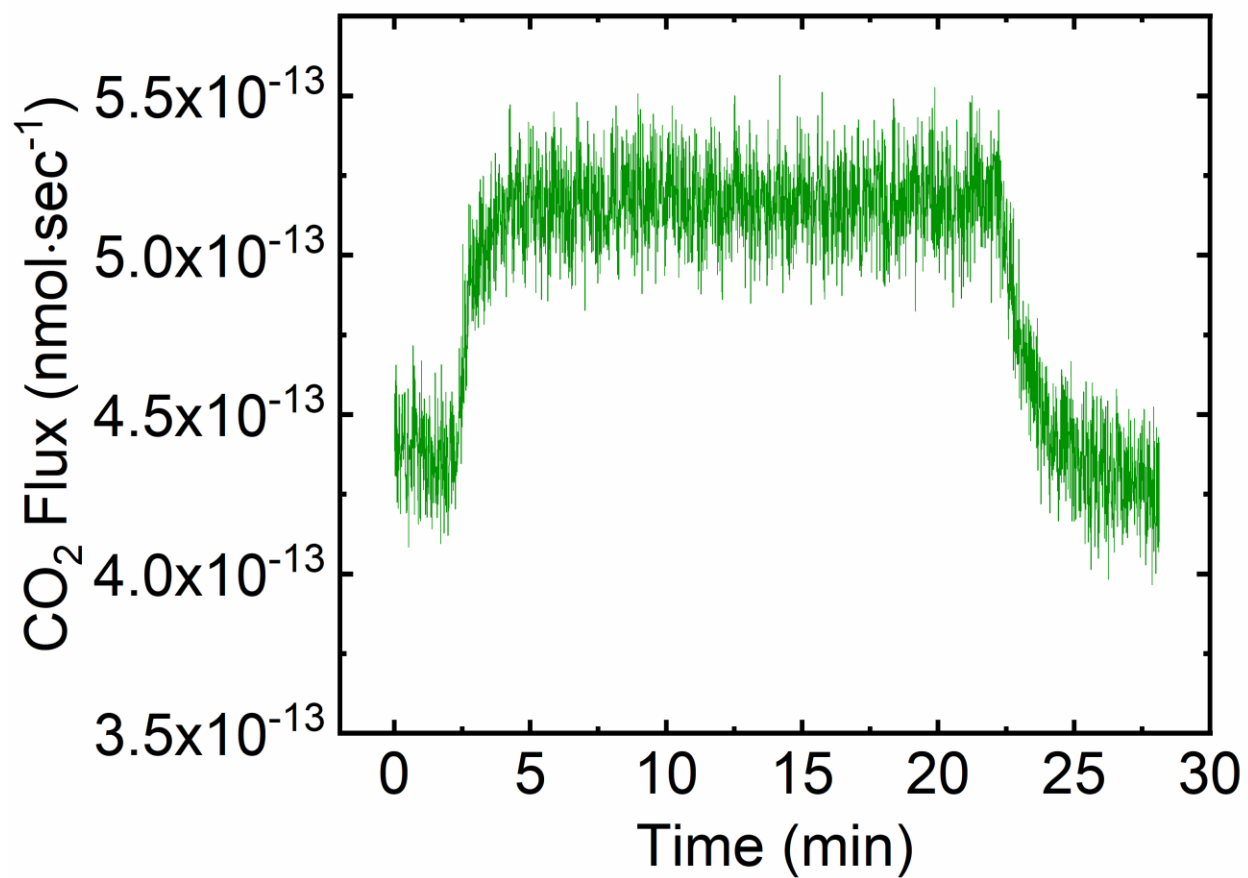


Figure S22. Carbon dioxide evolved during chronopotentiometry measurements of the electrode containing the mixed ionomer in 1 M KOH using a current density of 0.5 mA·cm⁻².

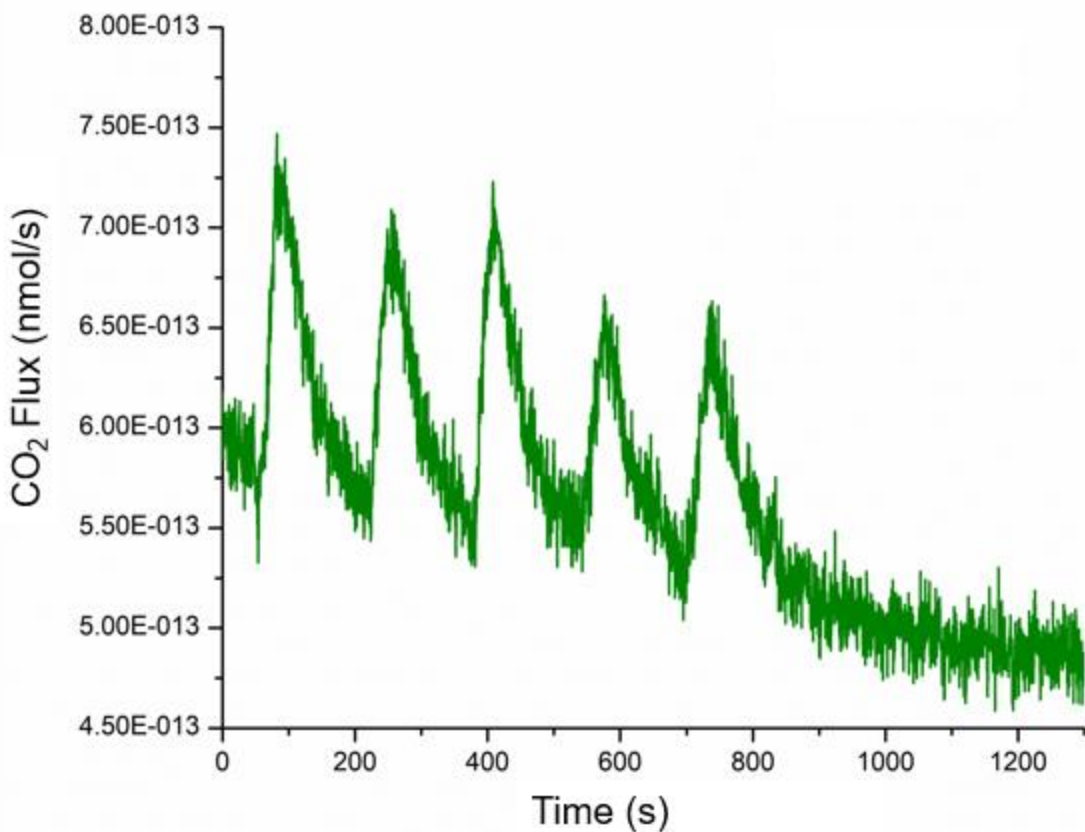


Fig. S23. Carbon dioxide evolved during cyclic voltammetry measurements of the electrode containing Nafion in 1 M KOH using a scan rate of $5 \text{ mV} \cdot \text{s}^{-1}$.

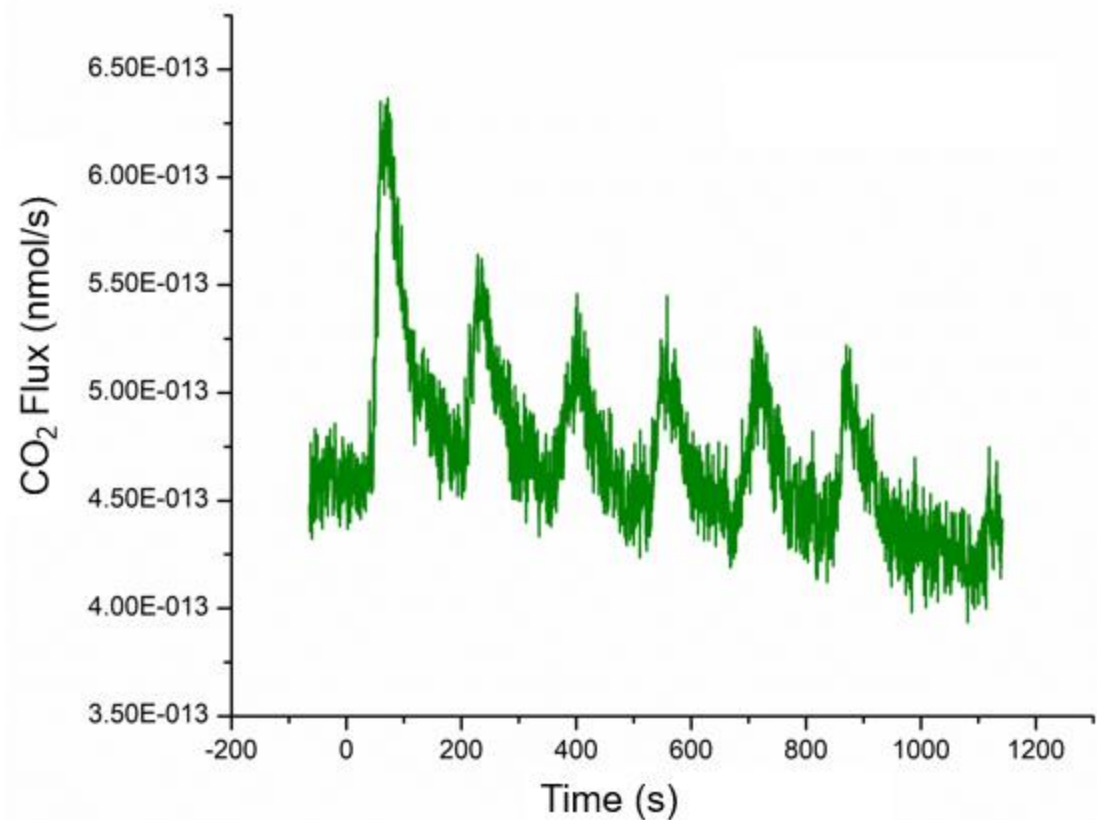


Fig. S24. Carbon dioxide evolved during cyclic voltammetry measurements of the electrode containing Fumion in 1 M KOH using a scan rate of $5 \text{ mV} \cdot \text{s}^{-1}$.

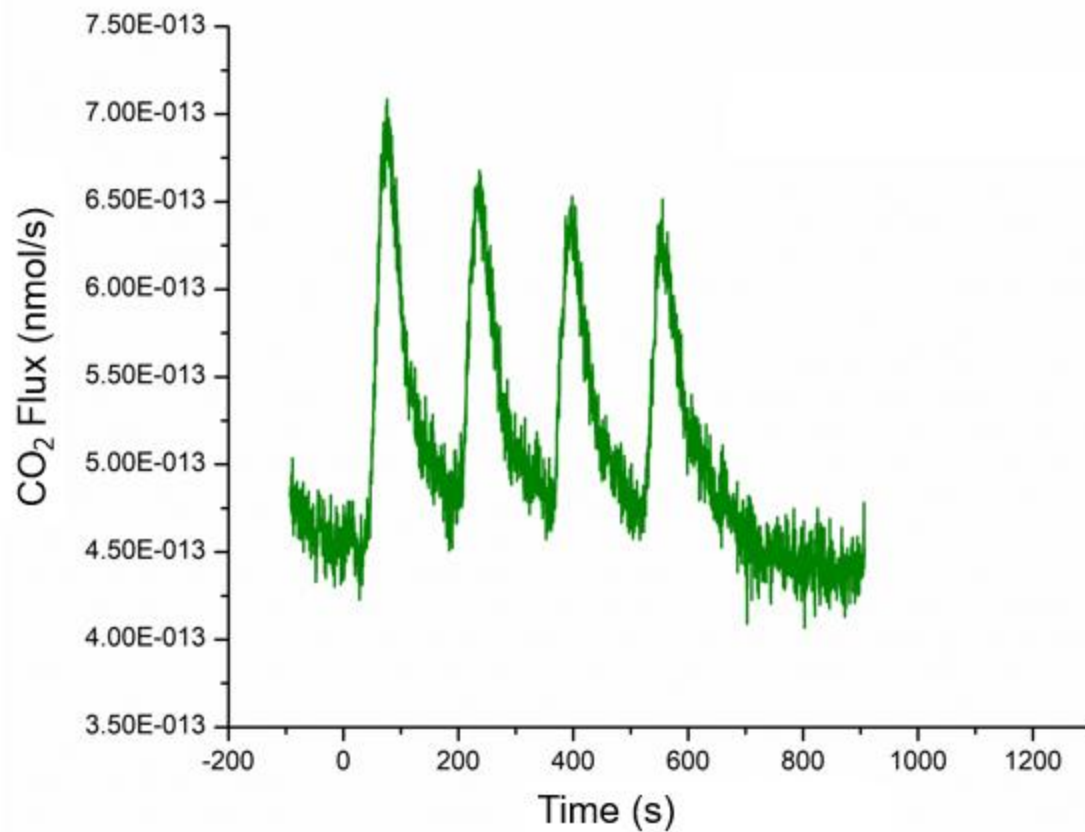


Fig. S25. Carbon dioxide evolved during cyclic voltammetry measurements of the electrode containing mixed ionomer in 1 M KOH using a scan rate of $5 \text{ mV}\cdot\text{s}^{-1}$.

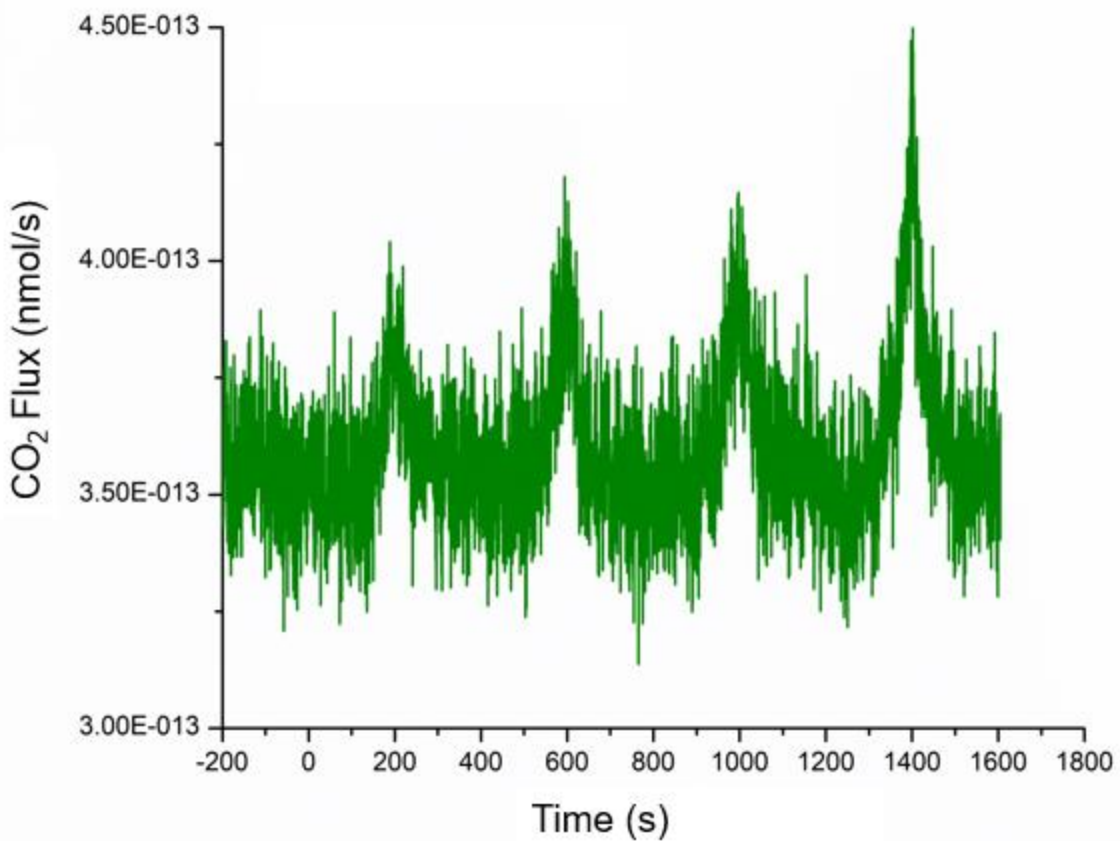


Fig. S26. Carbon dioxide evolved during cyclic voltammetry measurements of a bare glassy carbon electrode in 1 M KOH using a scan rate of $5 \text{ mV} \cdot \text{s}^{-1}$.

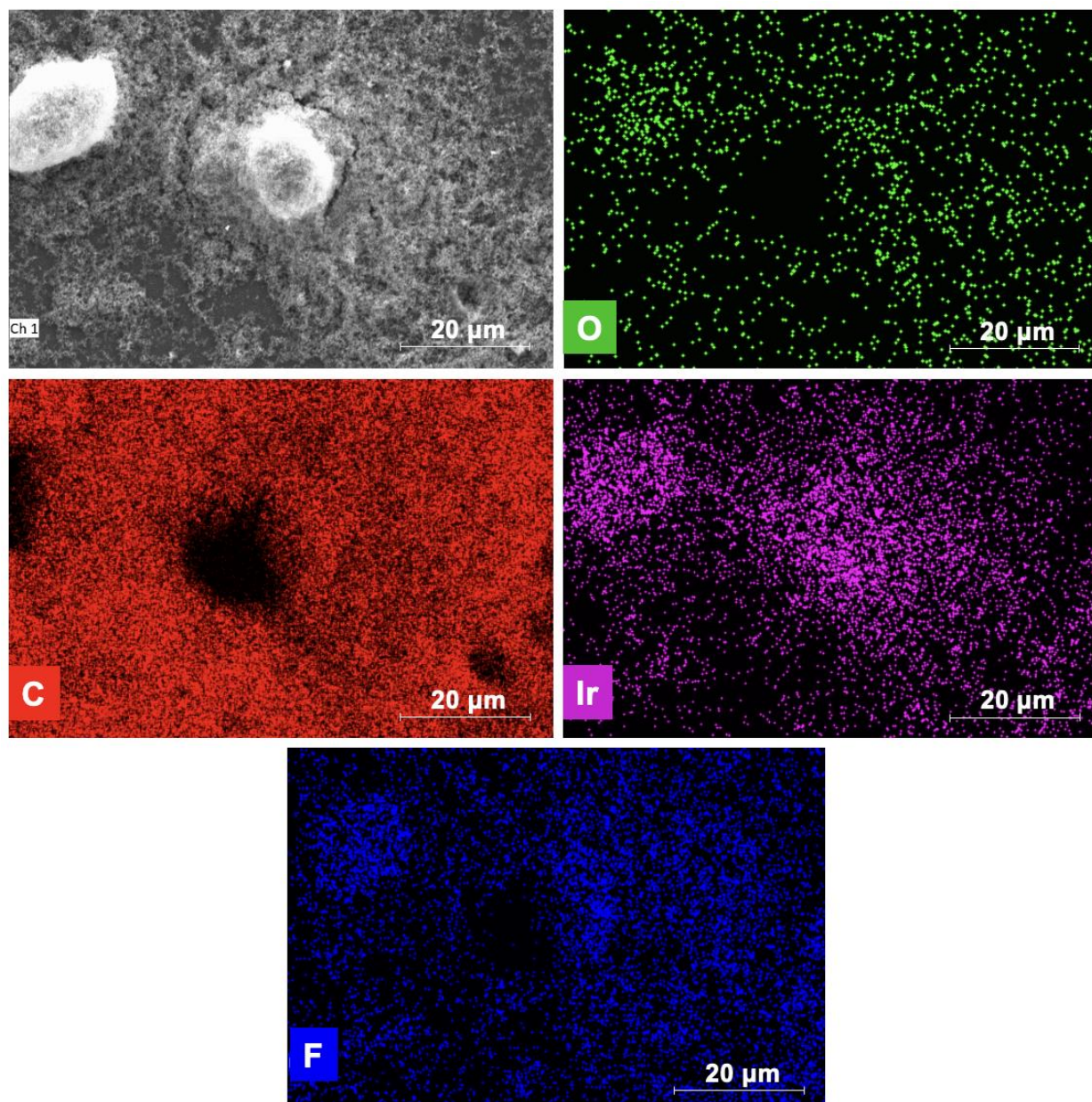


Fig. S27. EDS mapping images showing atomic composition of an electrode containing Ir/C and Nafion before exposing the sample to a current of $10 \text{ mA} \cdot \text{cm}^{-2}$ for 30 minutes.

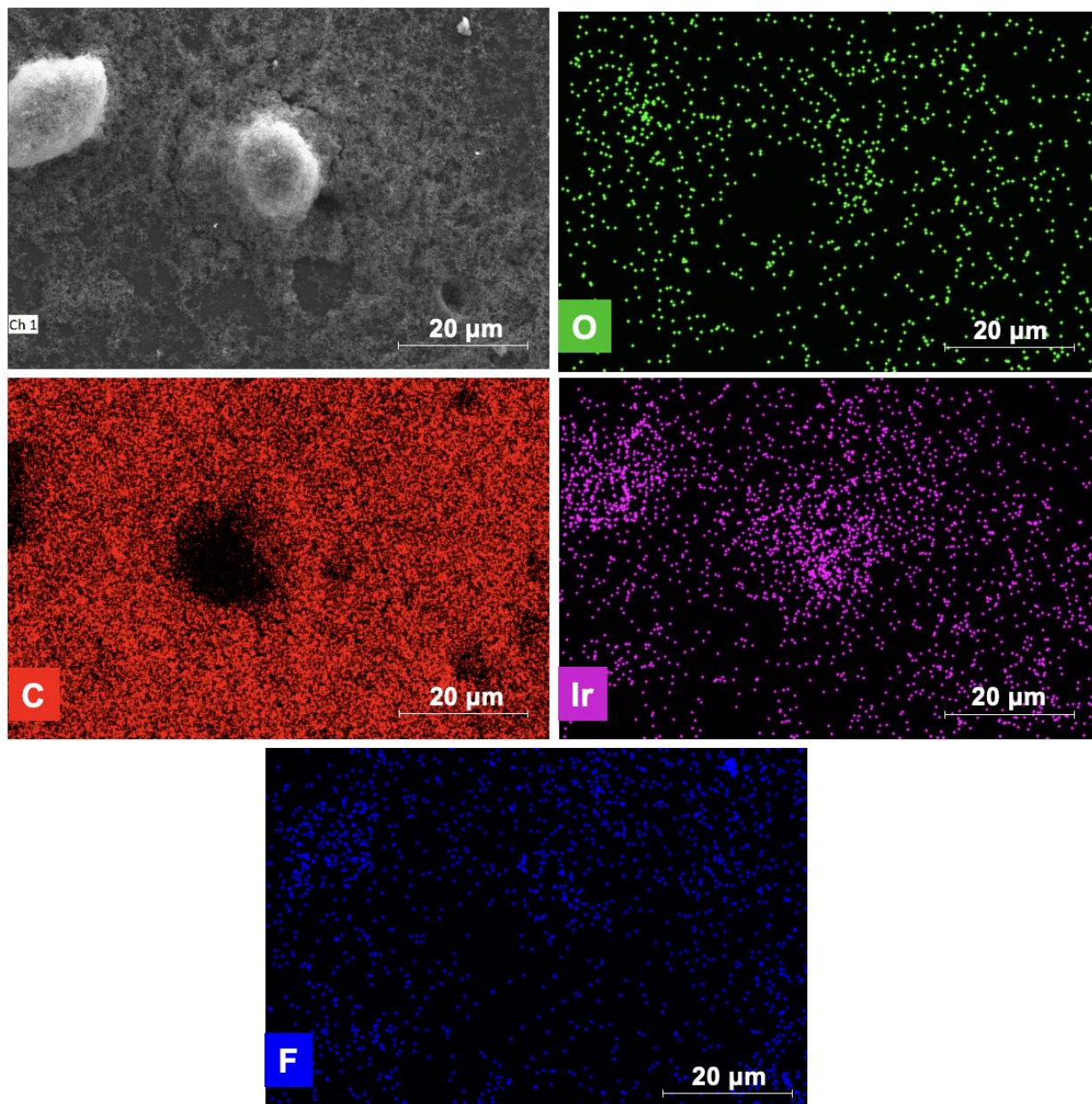


Fig. S28. EDS mapping images showing atomic composition of an electrode containing Ir/C and Nafion after exposing the sample to a current of $10 \text{ mA} \cdot \text{cm}^{-2}$ for 30 minutes.

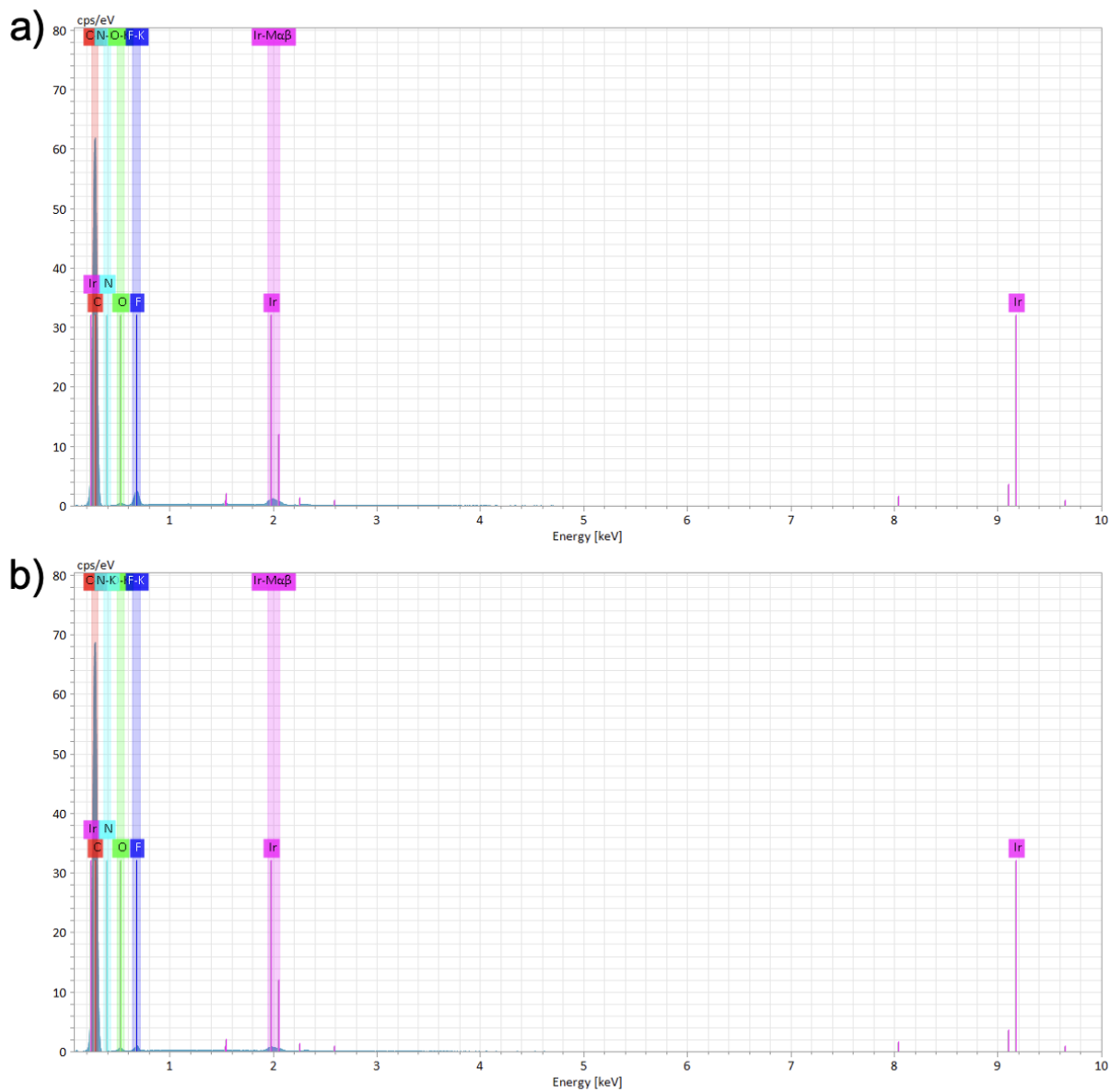


Fig. S29. EDS spectra of electrodes containing Nafion (a) before and (b) after being exposed to 10 mA·cm⁻² for 30 minutes.

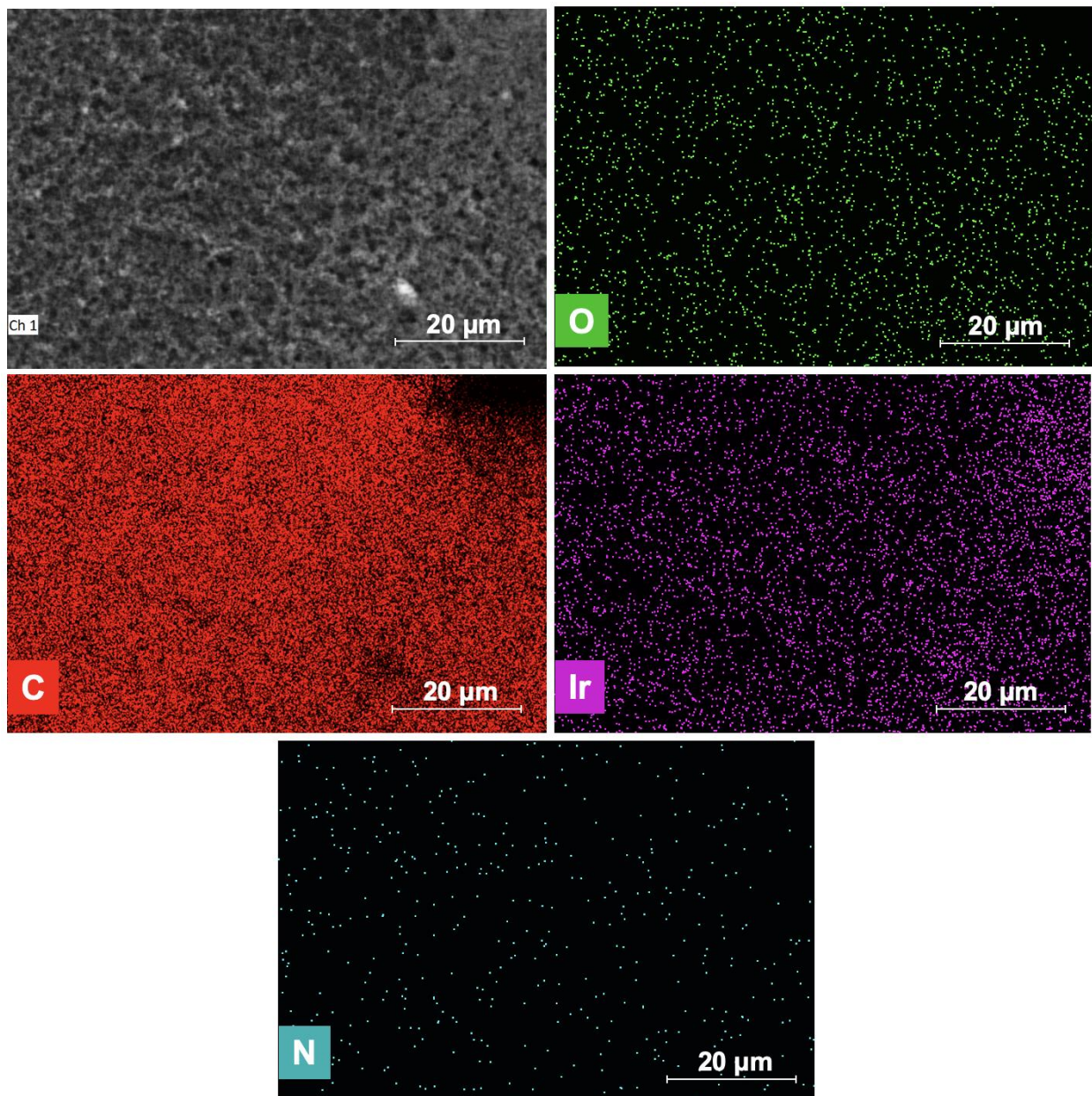


Fig. S30. EDS mapping images showing atomic composition of an electrode containing Ir/C and Fumion before exposing the sample to a current of $10 \text{ mA} \cdot \text{cm}^{-2}$ for 30 minutes.

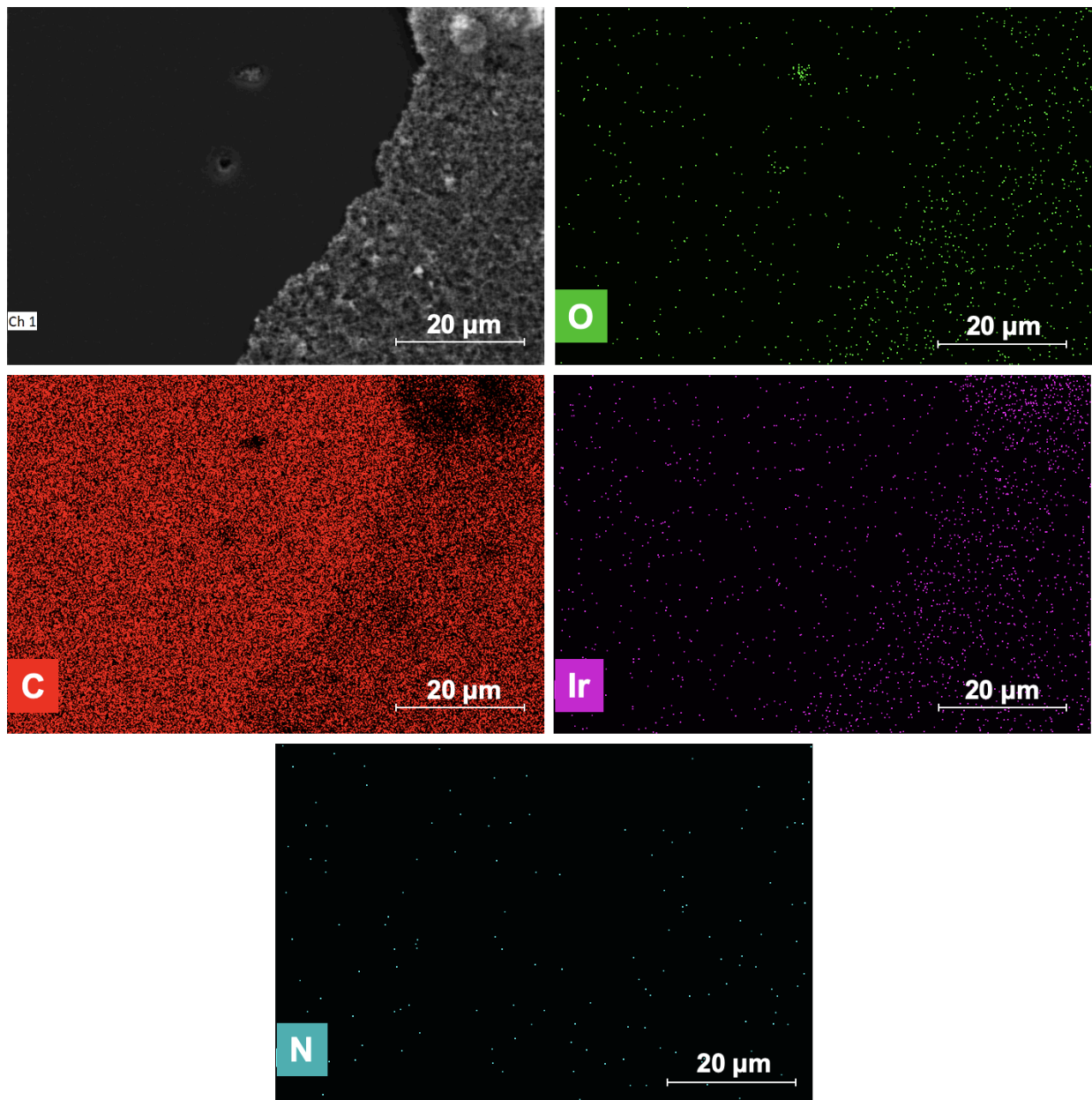


Fig. S31. EDS mapping images showing atomic composition of an electrode containing Ir/C and Fumion after exposing the sample to a current of $10 \text{ mA}\cdot\text{cm}^{-2}$ for 30 minutes.

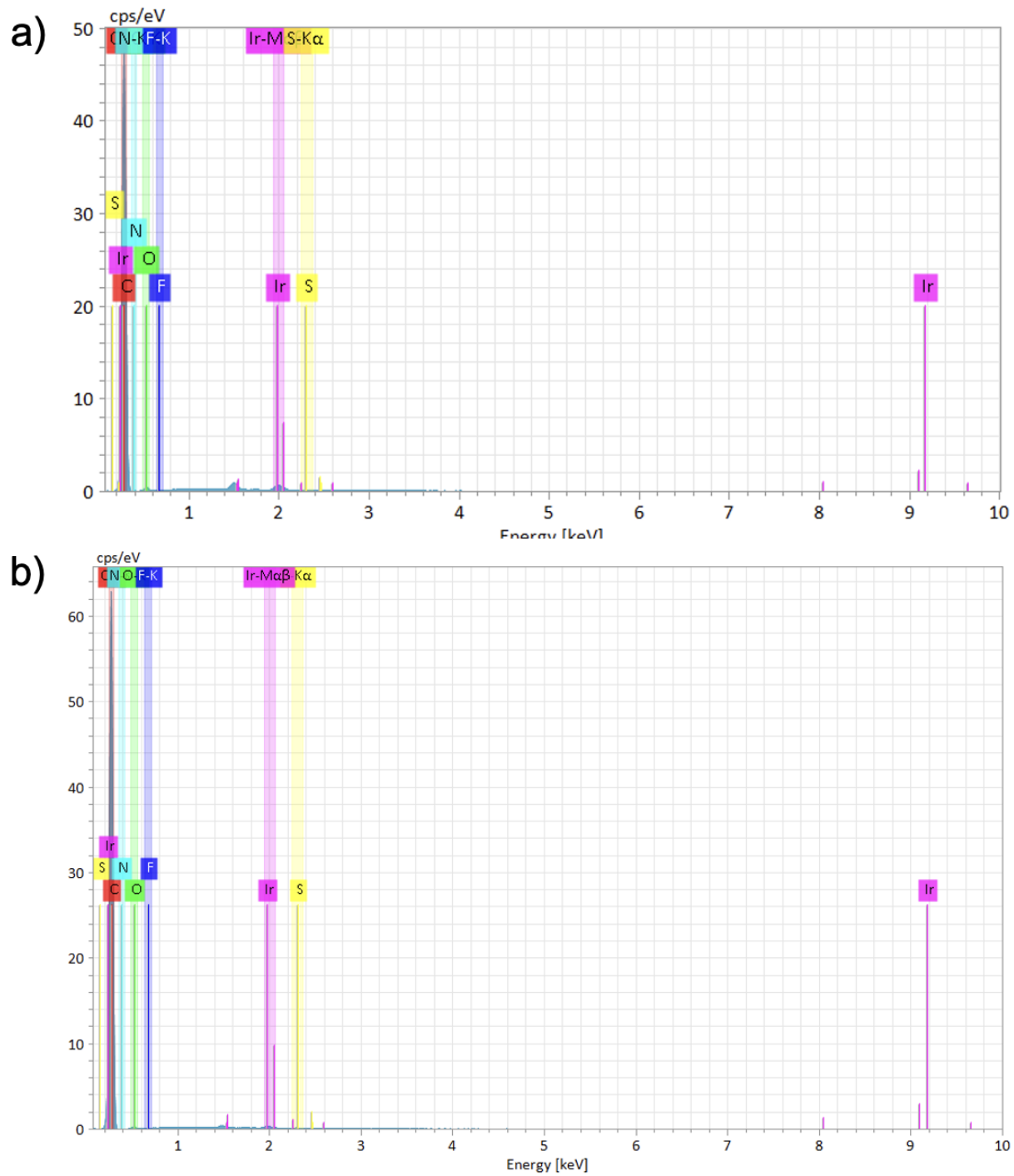


Fig. S32. EDS spectra of electrodes containing Fumion (a) before and (b) after being exposed to $10 \text{ mA} \cdot \text{cm}^{-2}$ for 30 minutes.

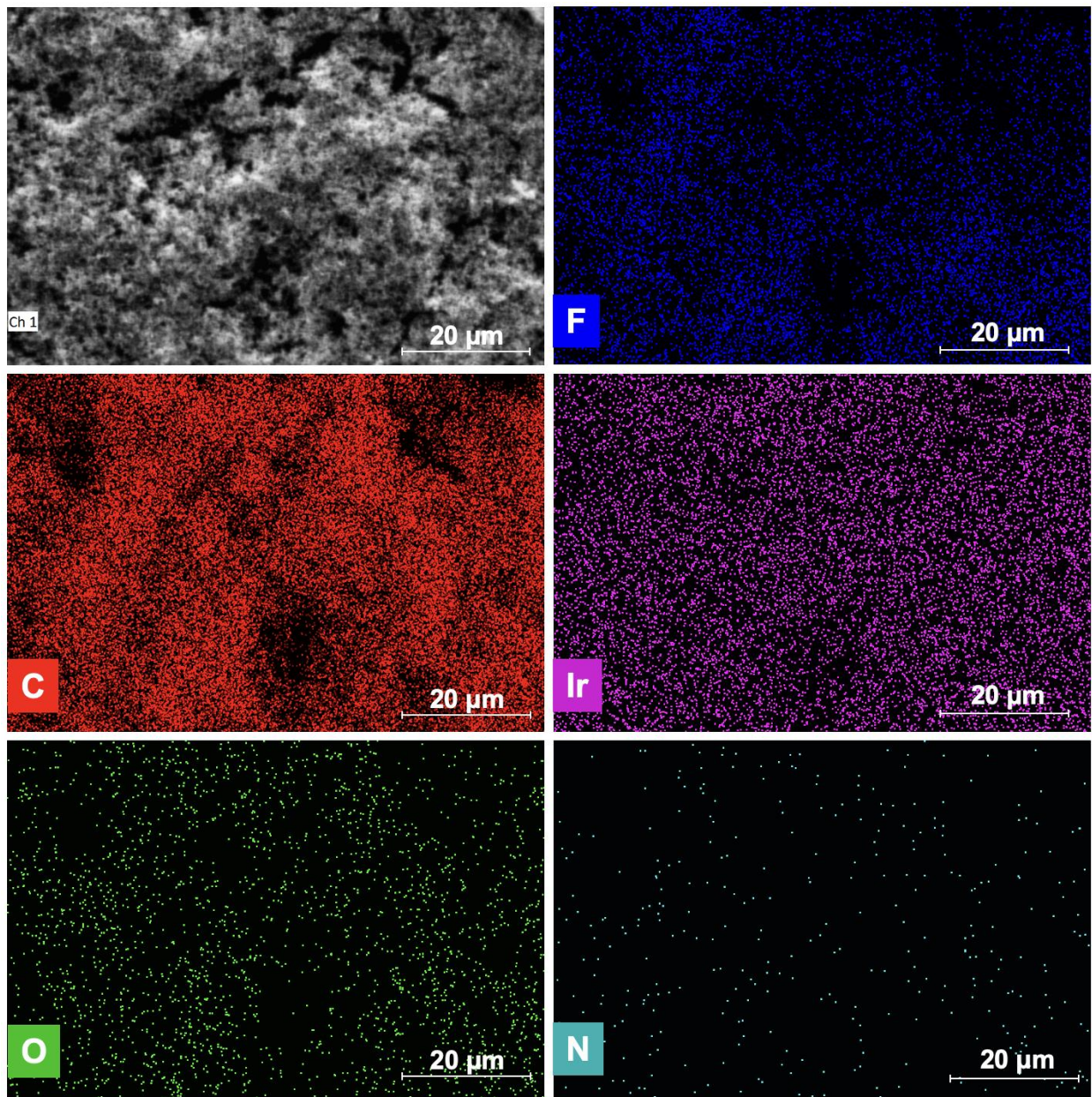


Fig. S33. EDS mapping images showing atomic composition of an electrode containing Ir/C and 1:1 Nafion:Fumion before exposing the sample to a current of $10 \text{ mA} \cdot \text{cm}^{-2}$ for 30 minutes.

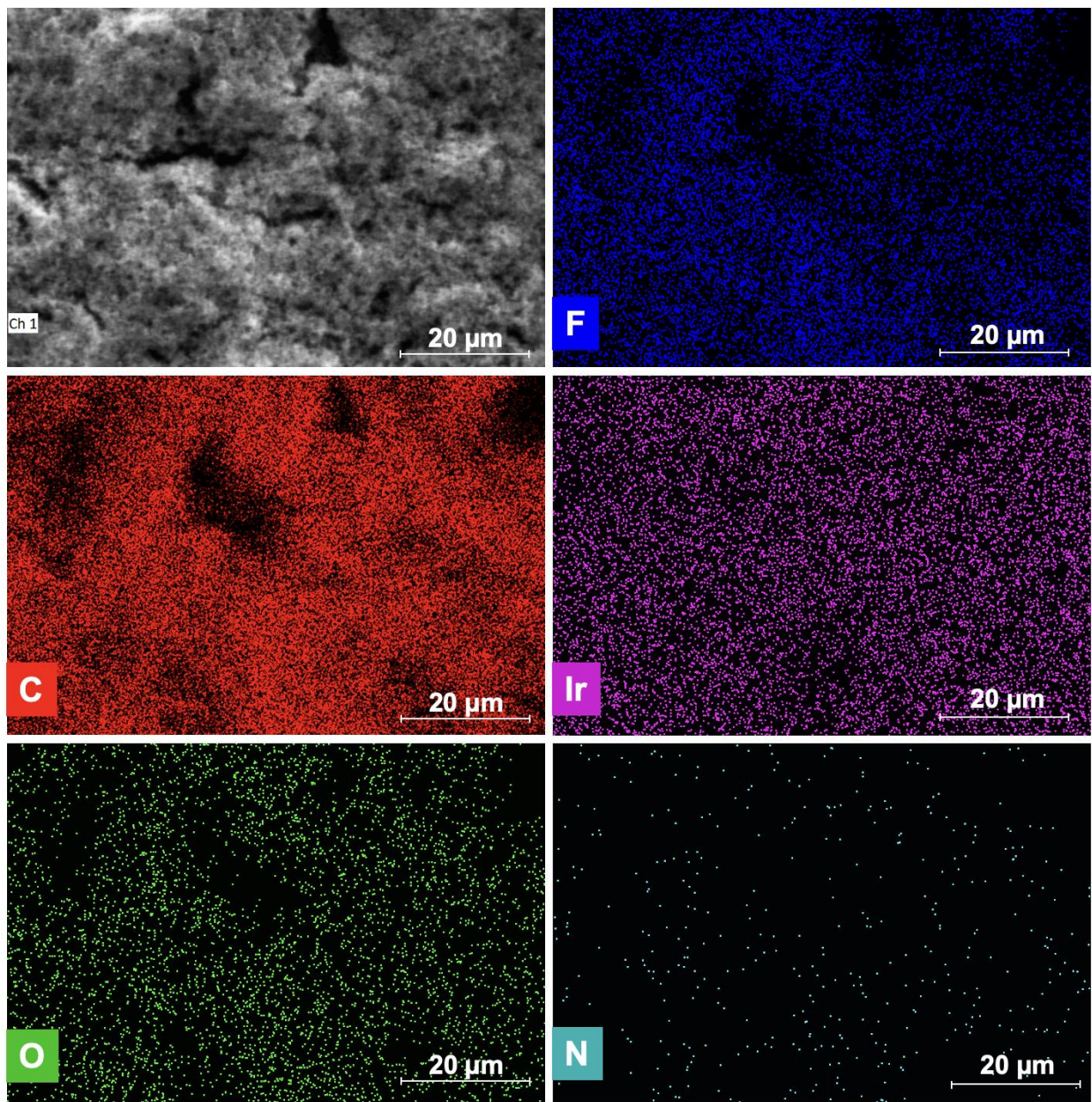


Fig. S34. EDS mapping images showing atomic composition of an electrode containing Ir/C and 1:1 Nafion:Fumion after exposing the sample to a current of $10 \text{ mA}\cdot\text{cm}^{-2}$ for 30 minutes.

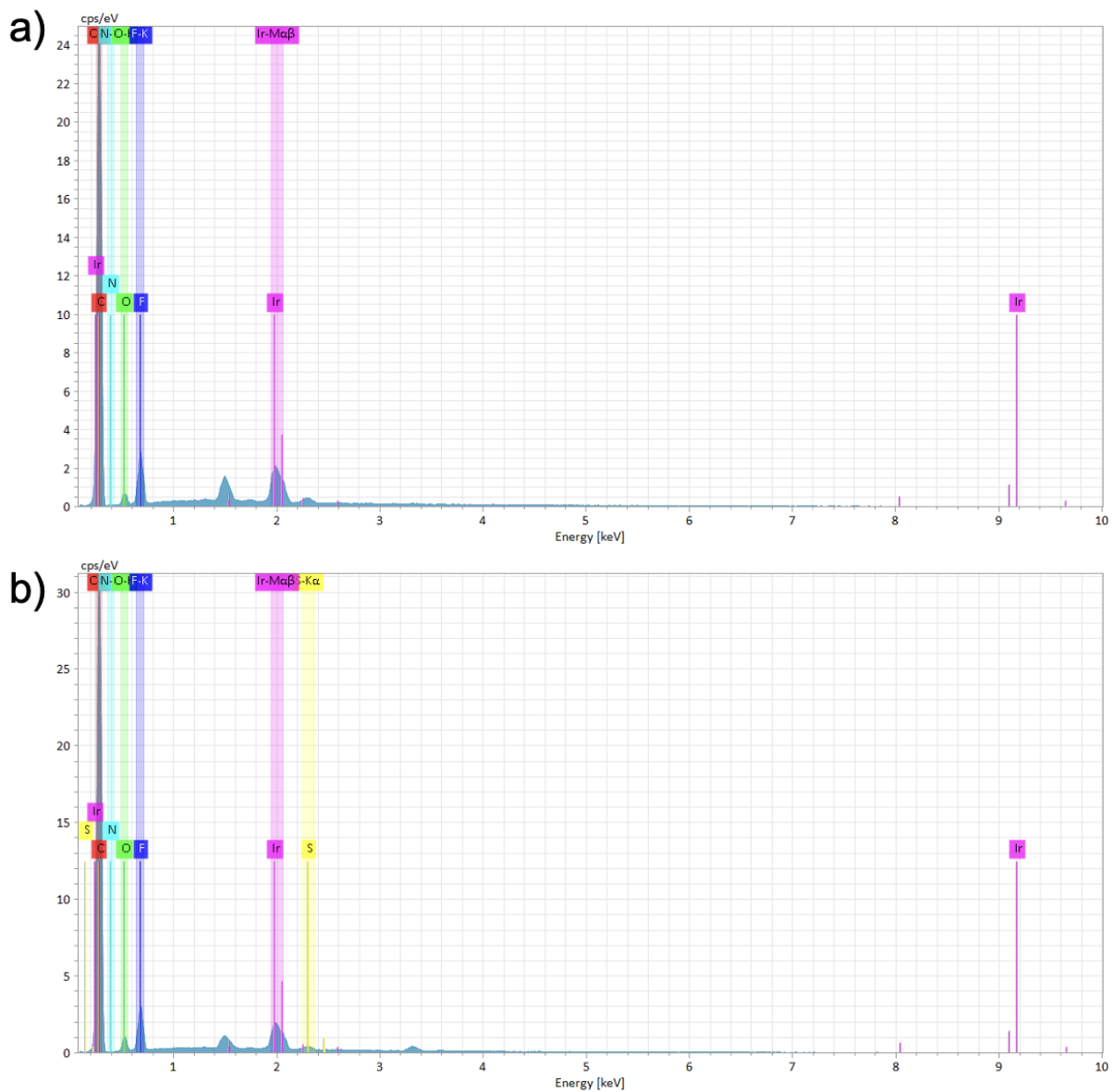


Fig. S35. EDS spectra of electrodes containing 1:1 Nafion:Fumion (a) before and (b) after being exposed to $10 \text{ mA} \cdot \text{cm}^{-2}$ for 30 minutes.

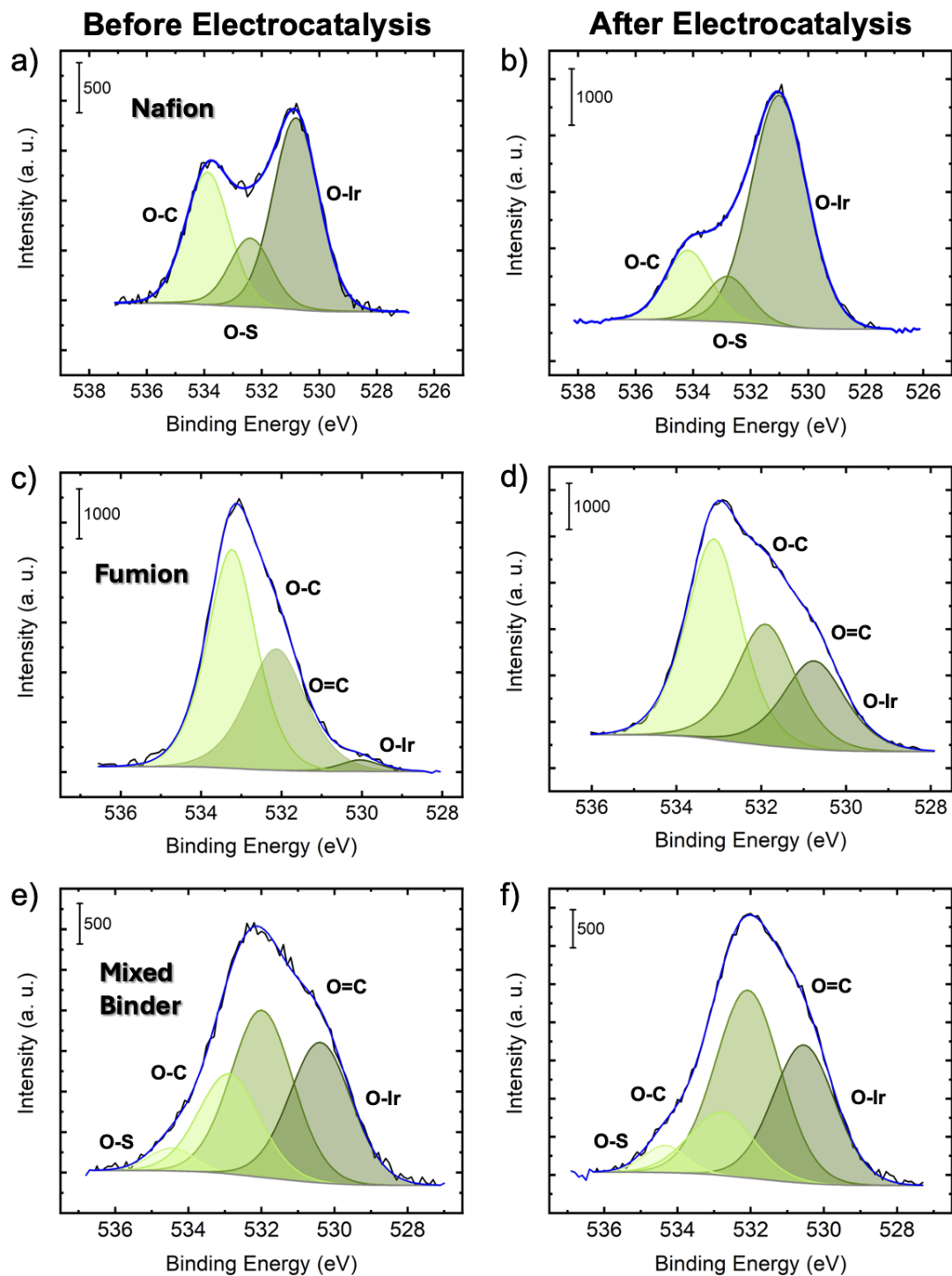


Fig. S36. O 1s XPS spectra of dropcasted Ir/C electrodes with (a, b) Nafion, (c, d) Fumion, and (e, f) mixed ionomer both before (a, c, e) and after (b, d, f) electrocatalysis performed in 1 M KOH at a current density of $10 \text{ mA} \cdot \text{cm}^{-2}$ for 30 minutes.

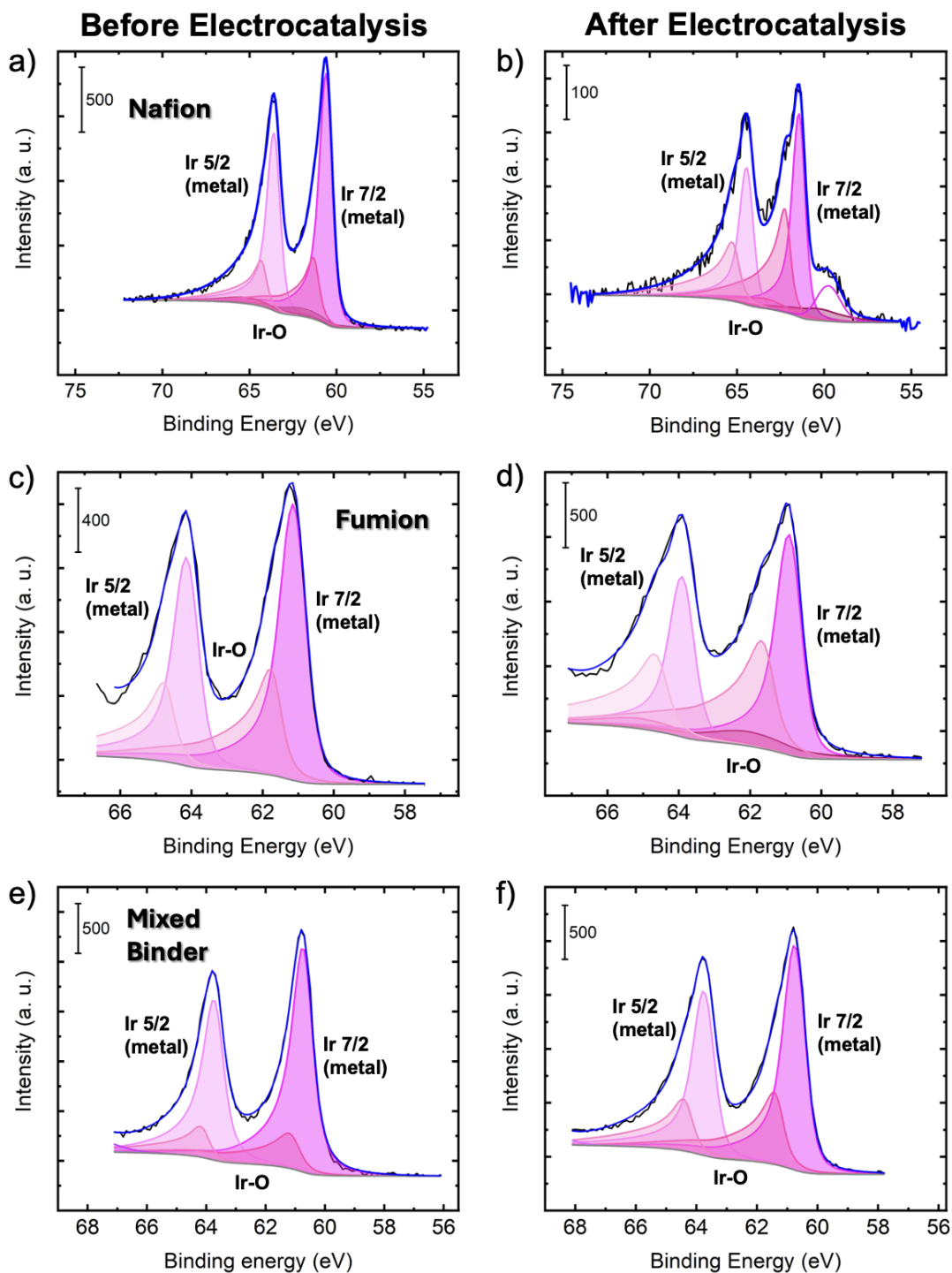


Fig. S37. Ir 4f XPS spectra of dropcasted Ir/C electrodes with (a, b) Nafion, (c, d) Fumion, and (e, f) mixed ionomer both before (a, c, e) and after (b, d, f) electrocatalysis performed in 1 M KOH at a current density of $10 \text{ mA} \cdot \text{cm}^{-2}$ for 30 minutes.

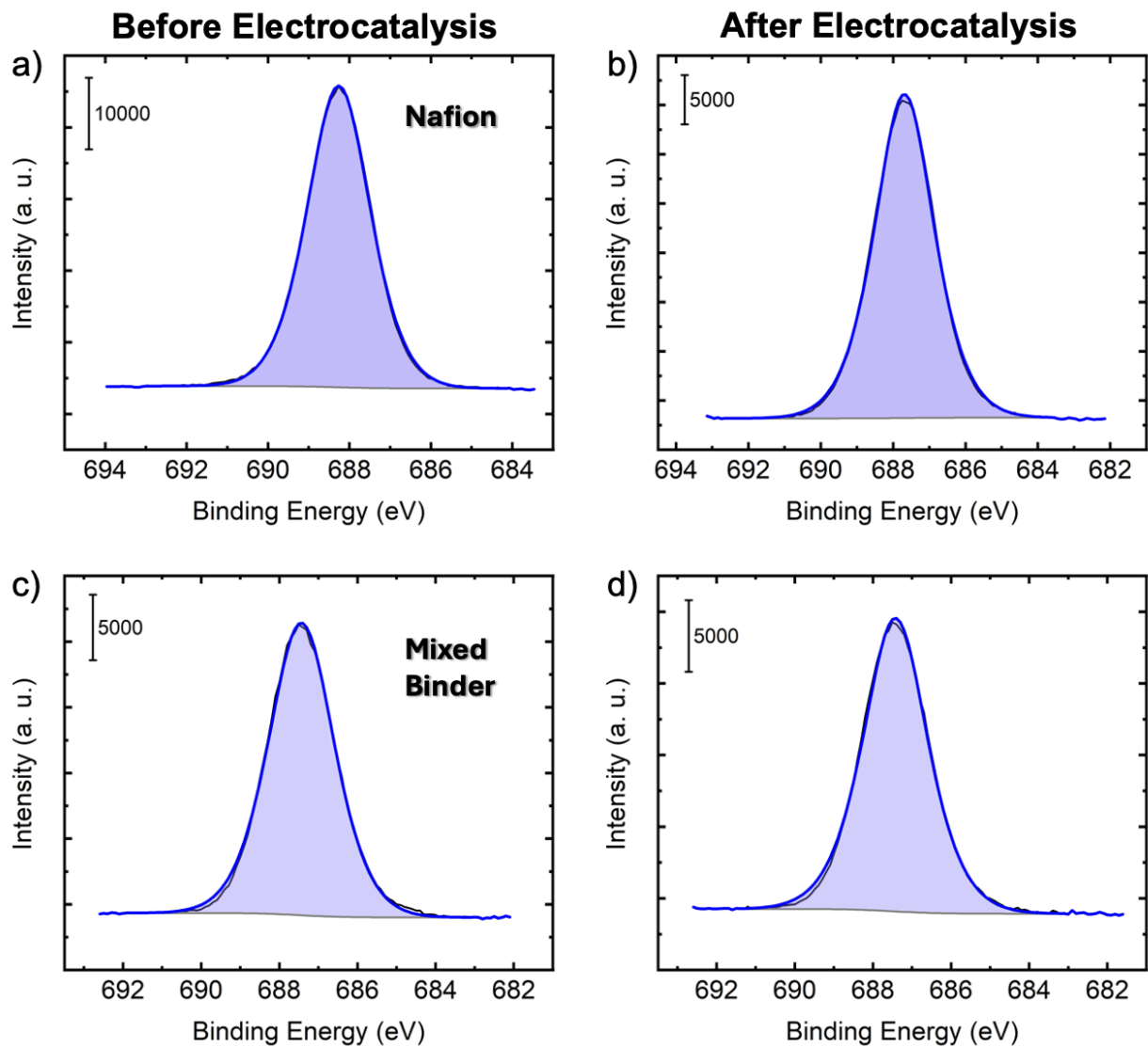


Fig. S38. F 1s XPS spectra of dropcasted Ir/C electrodes with (a, b) Fumion, (c, d) mixed ionomer both before (a, c) and after (b, d) electrocatalysis in 1M KOH at a current density of $10 \text{ mA} \cdot \text{cm}^{-2}$ for 30 minutes.

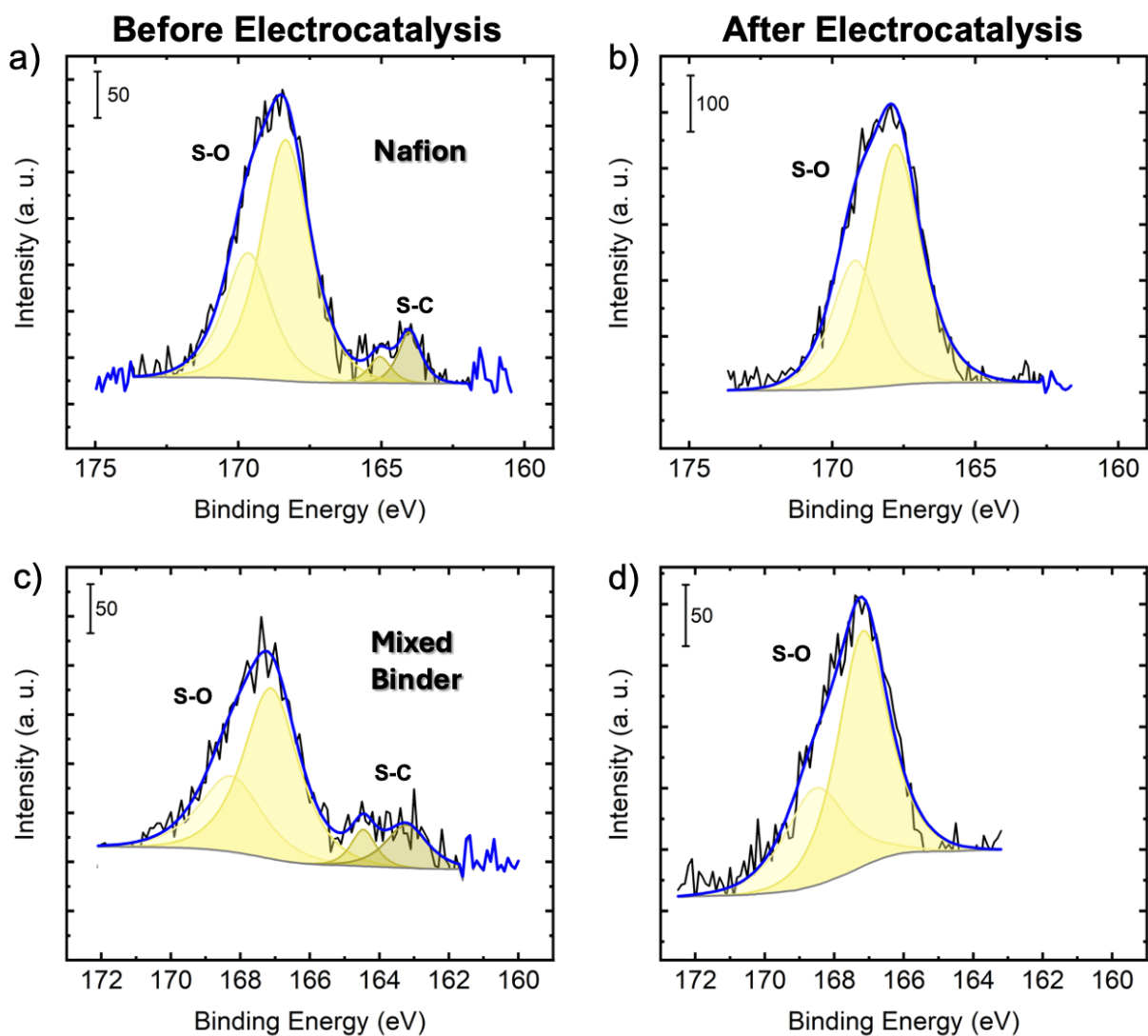


Fig. S39. S 2p XPS spectra of dropcasted Ir/C electrodes with (a, b) Fumion, (c, d) mixed ionomer both before (a, c) and after (b, d) electrocatalysis in 1 M KOH at a current density of $10 \text{ mA} \cdot \text{cm}^{-2}$ for 30 minutes.

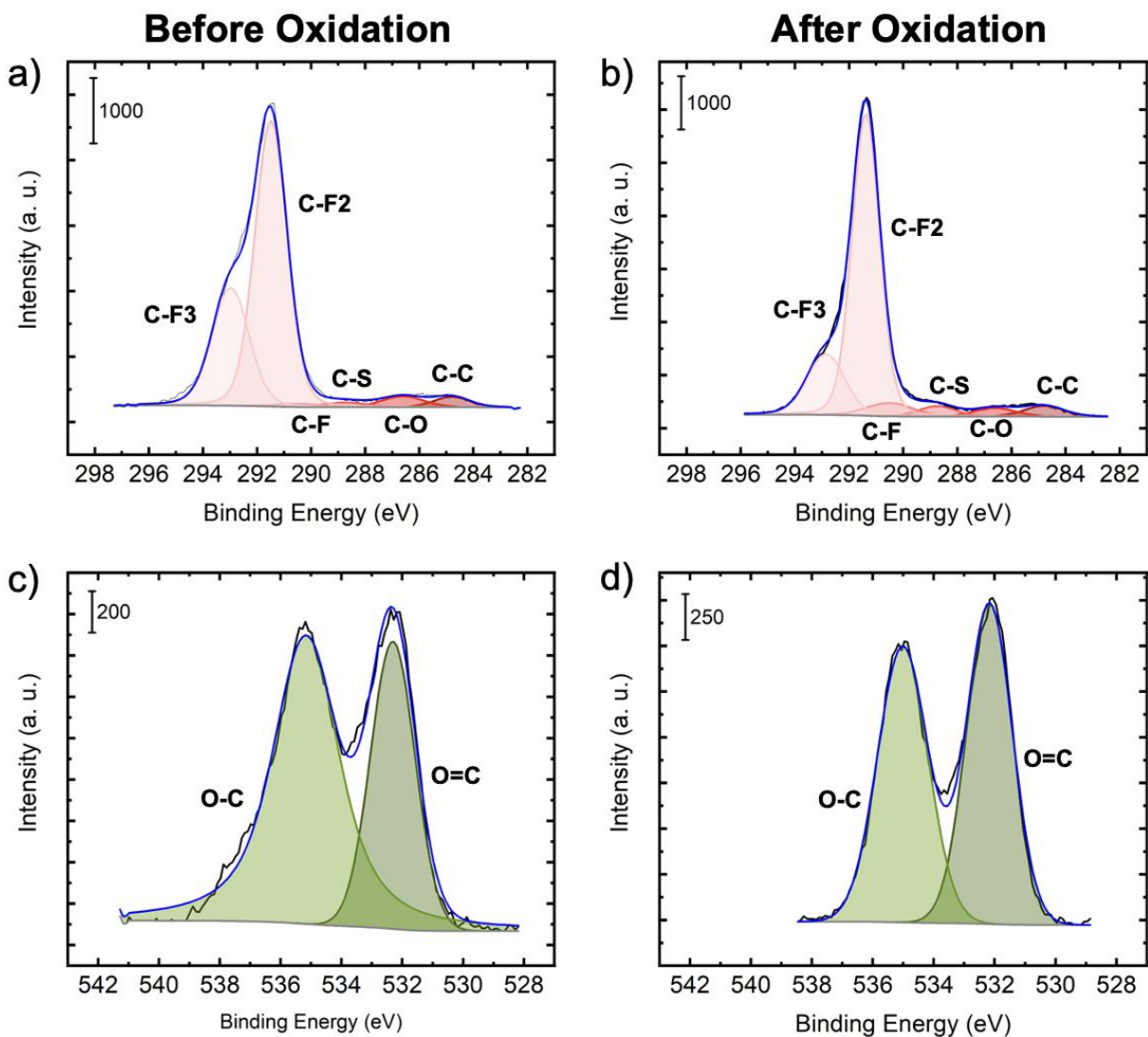


Fig. S40. (a, b) C 1s and (c, d) O 1s XPS spectra of dropcasted Nafion stock solution both before and after being exposed to oxidizing current in 1 M KOH at a current density of $10 \text{ mA}\cdot\text{cm}^{-2}$ for 30 minutes.

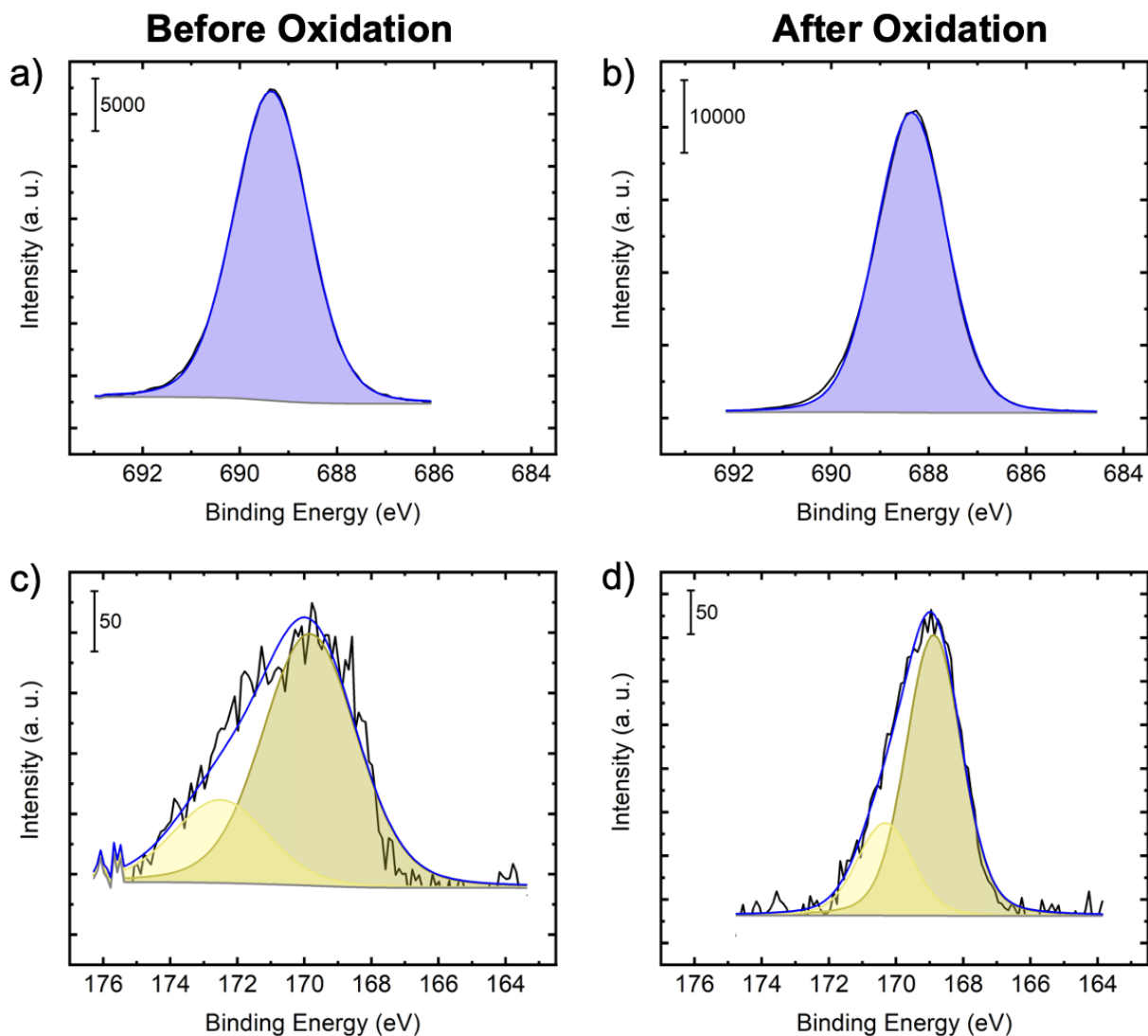


Fig. S41. (a, b) F 1s and (c, d) S 2p XP spectra of dropcasted Nafion stock solution both before and after being exposed to oxidizing current in 1 M KOH at a current density of $10 \text{ mA}\cdot\text{cm}^{-2}$ for 30 minutes.

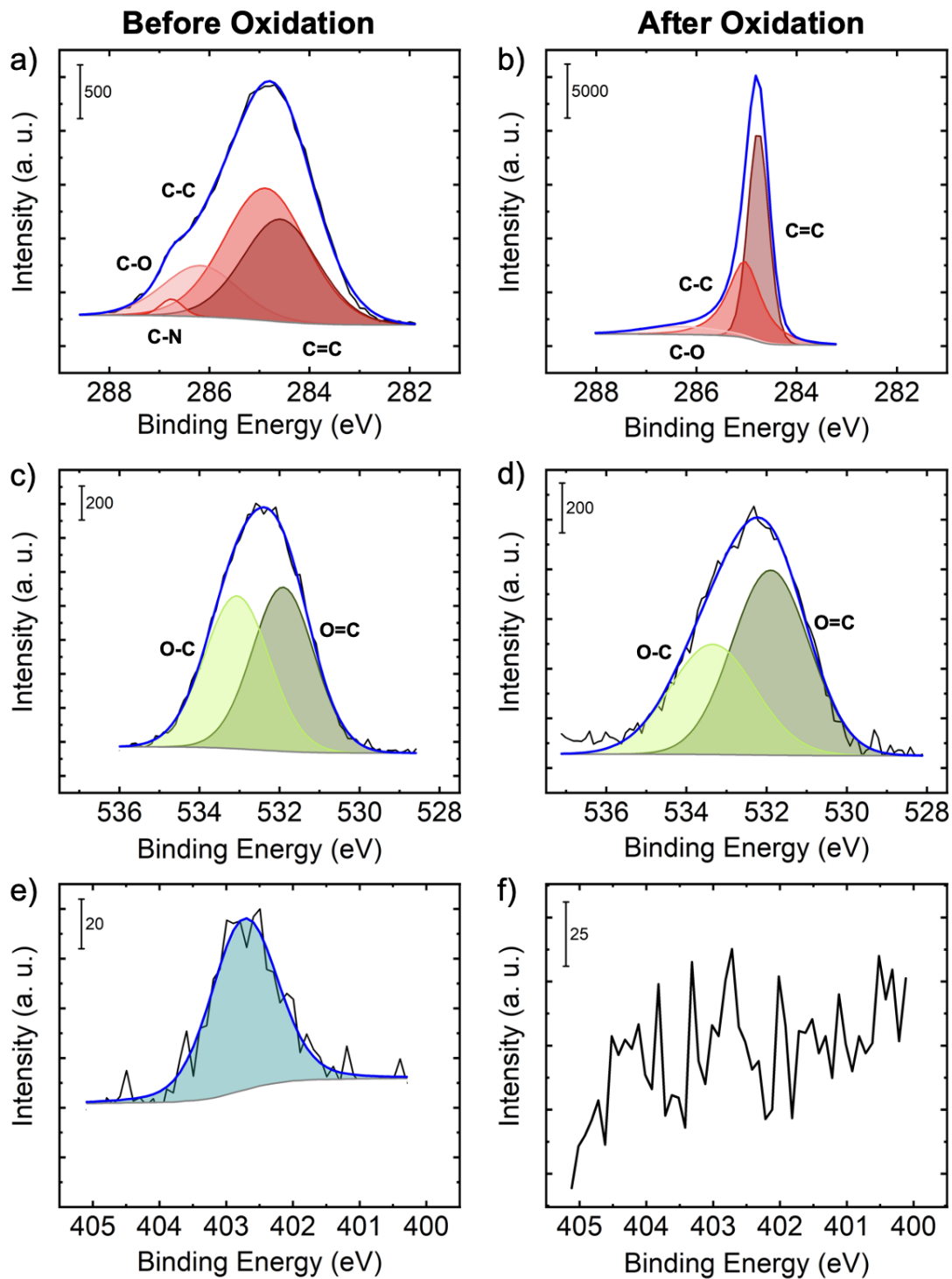


Fig. S42. (a, b) C 1s, (c, d) O 1s, and (e, f) N 1s XPS spectra of dropcasted Fumion stock solution both before and after being exposed to oxidizing current in 1 M KOH at a current density of 10 mA·cm⁻² for 30 minutes.

References

- 1 M. K. Horton, P. Huck, R. X. Yang, J. M. Munro, S. Dwaraknath, A. M. Ganose, R. S. Kingsbury, M. Wen, J. X. Shen, T. S. Mathis, A. D. Kaplan, K. Berket, J. Riebesell, J. George, A. S. Rosen, E. W. C. Spotte-Smith, M. J. McDermott, O. A. Cohen, A. Dunn, M. C. Kuner, G.-M. Rignanese, G. Petretto, D. Waroquiers, S. M. Griffin, J. B. Neaton, D. C. Chrzan, M. Asta, G. Hautier, S. Cholia, G. Ceder, S. P. Ong, A. Jain and K. A. Persson, *Nat. Mater.*, 2025, **24**, 1522–1532.
- 2 A. Jain, S. P. Ong, G. Hautier, W. Chen, W. D. Richards, S. Dacek, S. Cholia, D. Gunter, D. Skinner, G. Ceder and K. A. Persson, *APL Mater.*, 2013, **1**, 011002.
- 3 A. M. Patel, J. K. Nørskov, K. A. Persson and J. H. Montoya, *Phys. Chem. Chem. Phys.*, 2019, **21**, 25323–25327.
- 4 A. K. Singh, L. Zhou, A. Shinde, S. K. Suram, J. H. Montoya, D. Winston, J. M. Gregoire and K. A. Persson, *Chem. Mater.*, 2017, **29**, 10159–10167.
- 5 K. A. Persson, B. Walwick, P. Lazic and G. Ceder, *Phys. Rev. B*, 2012, **85**, 235438.